

# Assessing the importance of conditioning factor selection in Landslide Susceptibility for Belluno province (Veneto Region, NE Italy)

Sansar Raj Meena<sup>1,2</sup> \*, Silvia Puliero<sup>1</sup>, Kushanav Bhuyan<sup>1,2</sup>, Mario Floris<sup>1</sup>, Filippo Catani<sup>1</sup>

<sup>1</sup> Department of Geosciences, University of Padova, Padova, Italy.

<sup>2</sup> Faculty of Geo-Information Science and Earth Observation (ITC), University of Twente, Enschede, Netherlands.

\* Corresponding author Email: sansarraaj.meena@unipd.it

## Abstract

In the domain of landslide risk science, landslide susceptibility mapping (LSM) is very important as it helps spatially identify potential landslide-prone regions. This study used a statistical ensemble model (Frequency Ratio and Evidence Belief Function) and two machine learning (ML) models (Random Forest and XG-Boost) for LSM in the Belluno province (Veneto Region, NE Italy). The study investigated the importance of the conditioning factors in predicting landslide occurrences using the mentioned models. In this paper, we evaluated the importance of the conditioning factors in the overall prediction capabilities of the statistical and ML algorithms. By the trial-and-error method, we eliminated the least "important" features by using a common threshold of 0.30 for statistical and 0.03 for ML algorithms. Conclusively, we found that removing the least "important" features does not impact the overall accuracy of the LSM for all three models. Based on the results of our study, the most commonly available features, for example, the topographic features, contributes to comparable results after

removing the least "important" ones, namely aspect plan and profile curvature, TWI, TRI and NDVI, in the case of statistical model and plan and profile curvature, TWI and TPI for ML algorithms. This confirms that the requirement for the important conditioning factor maps can be assessed based on the physiography of the region.

## 1. Introduction

Landslides are one of the most frequently occurring natural disasters that cause significant human casualties and infrastructure destruction (Froude and Petley 2018). Landslides are triggered by several natural and man-made events such as earthquakes, volcanic eruptions, heavy rains, extreme winds, and unsustainable construction activities such as unplanned settlement development and cutting of roads along the slopes (Glade et al., 2006; van Westen et al., 2008). Extreme meteorological events such as the Vaia storm of 2018 triggered landslides and debris flow, destroyed critical infrastructures in the northern parts of Italy (Boretto et al., 2021). As reported by (Gariano et al., 2021) in the last 50 years between 1969-2018, landslides posed a severe threat to the Italian population. Approximately, 1500 out of the 8100 municipalities in Italy have faced landslides with severe fatalities. Between the years of 1990 and 1999, 263 people were killed by landslides. Studies by (Rossi et al., 2019) estimated that approximately 2500 people were killed between 1945-1990. Moreover, predictive modelling of the Italian population at risk to landslides (Rossi et al., 2019) shows massive tendency of risk to the population with data acquired between 1861-2015, emphasizing the necessity for landslide risk studies.

Therefore, to assess landslide risk and to plan for risk mitigation measures, it is crucial to analyse the Landslide susceptibility Mapping (LSM). LSM is an essential tool that incorporates potential landslide locations (Senouci et al., 2021). The probability of a landslide occurring in a particular region owing to the effects of several causative factors is referred to as landslide

susceptibility (Reichenbach et al. 2018). LSM is an essential step towards landslide risk management and helps in effective mapping of the spatial distribution of probable landslide manifestations (Dai et al., 2002). In the past, researchers have used a range of models to assess landslide susceptibility using technologies such as Earth Observation (EO) and Geographic Information Systems (GIS). The recognition and analysis of slope movements have been going on since the early 1970s (Brabb et al., 1972) and is still one of the most important components to perform LSM (Ercanoglu and Gokceoglu, 2002; Chacón et al., 2006; Guzzetti et al., 2006; Castellanos Abella and Van Westen, 2008; Floris et al., 2011; Catani et al., 2013; Pham et al., 2015; Reichenbach et al., 2018; Youssef and Pourghasemi, 2021; Liu et al., 2021). Traditional methods such as the expert-based Analytical Hierarchy Process (AHP), multi-variate statistics, data-driven have been employed for landslide susceptibility for many years, with satisfactory results (Pradhan, 2010; Castellanos Abella and Van Westen, 2008; Komac, 2006). A use case of such approaches is given by Floris et al (2011) which apply traditional LSM methods (FR) for mapping landslide susceptibility in a case study in Veneto Region, Italy. Afterwards, with the development of new approaches, susceptibility modelling has advanced from traditional approaches. Presently, two approaches: (1) statistical and (2) machine learning, are practised for LSM at investigating the landslide predisposing factors and to map the geographical distribution of landslide processes. (Reichenbach et al., 2018) classified landslide susceptibility models into six main groups: (1) classical statistics, (2) index-based, (3) machine learning, (4) multi-criteria analysis, (5) neural networks, and (6) others. Research by (Reichenbach et al., 2018) also depicted that before 1995, only five models were used for LSM, but in recent times, an investigation of 19 other models was carried out, which yielded good results. More than 50 per cent of the methods consisting of the first five models mentioned above accounted for landslide susceptibility studies. Recent work of (Stanley et al., 2021) emphasized the importance of data-driven methods in global LSM, trained to report

76 landslide spatial occurrences between the periods of 2015-2018. The first version of the  
77 Landslide Hazard Assessment for Situational Awareness (LHASA) from their work for NASA,  
78 reported landslide occurrences with a decision tree model that first defines the intensity of one  
79 week of rainfall. LHASA version 2 used the data-driven model of XG-Boost by adding two  
80 dynamically varying factors: snow and soil moisture. However, despite advances in LSM, the  
81 importance of the conditioning factors in the prediction capability of a model is not discussed  
82 enough. The need of increasing our control over the model sensitivity to system parameters  
83 changes, including those induced by anthropogenic and climate-change dynamics, is becoming  
84 a key factor in the implementation of truly efficient LSM for risk mitigation purposes. The  
85 Vaia windstorm of 2018 (Forzieri et al., 2020), as a typical extreme weather event, may easily  
86 escape traditional statistical prediction schemes and represent, therefore, a challenging test for  
87 exploring the sensitivity of the various LSM models to changing factors and conditions.

88 One goal of this research is to look into the relative changes in LSM accuracy when the least  
89 "important" conditioning factors are removed. Feature selection in LSM is an approach in  
90 reducing landslide conditioning factors to improve model performance and reduce  
91 computational time. The purpose of this approach is to find the optimal set of conditioning  
92 factors that will provide the best fit for the model to yield higher accuracy as predictions.  
93 (Micheletti et al., 2014) emphasized the importance of feature selection in LSM and discussed  
94 the use of Machine Learning (ML) models such as Support Vector Machine (SVM), Random  
95 Forest (RF), and AdaBoost for LSM, as well as the significance of associated features within  
96 the confluence of the ML models for feature importance. However, their study did not consider  
97 geological and meteorological features like lithology, land use, and rainfall intensity for both  
98 LSM and feature selection. Studies by (Liu et al., 2021) depicted the improvement in the  
99 predictive capability of the so-called Feature Selected Machine Learning (FS-ML) model but  
100 also remarked on the fact that the same conditioning factors may contribute differently in

different ML models. In this study, we want to investigate the prediction capability of the model after removing conditioning factors as an approach to improve LSM accuracy in contrast to what has been done in literature like (Liu et al., 2021), where they assess conditioning factor importance using approaches like multi-collinearity analysis, variance inflation factor before prediction of the susceptibility. The identification of the most crucial features can help in monitoring the effect of extreme events (such as Vaia) on the changes in the evolution of landslide hazard.

We present a study in the province of Belluno (Veneto Region, NE Italy) with the comparison of the conditioning factor importance of statistical and ML models for LSM before the Vaia storm event. The results from the LSM will be then validated using the IFFI landslide inventory data for testing the various models' prediction capability with/without certain factors. We also investigate whether many of the latter conditioning factors are crucial for LSM. As in many regions over the world, the same data or factor maps might not be available.

## 2. Study area and Data

### 2.1 Study area

The area of the Belluno Province (Veneto Region, NE Italy) is part of the tectonic unit of the Southern Alps. The territory is 3,672 km<sup>2</sup> wide, stretching from north to south between the Dolomite Alps and the Venetian Pre-Alps, with elevations ranging from 42 to 3325 m above mean sea level. From a geological point of view, Dolomite Alps comprises the Hercynian crystalline basement consisting of micaschists and phyllites intruded by the Permian ignimbrites (Doglioni, 1990; Schönborn, 1999). These Paleozoic units are mainly outcropping in the NE and central-West sectors. The Middle-Upper Triassic includes carbonate, volcanic and dolomitic formations. In particular, the Upper Triassic Main Dolomite covers 14% of the whole province. Jurassic-Cretaceous limestone and marls are especially located between the

126 Valsugana and Belluno thrusts (Sauro et al., 2013). Moreover, in the Belluno valley and in the  
127 southern part of the area, Cenozoic sediments, i.e., flysch and molasse and Quaternary glacial,  
128 alluvial and colluvial deposits are largely present. Instead, Venetian Prealps are characterized  
129 by Jurassic-Cretaceous sedimentary cover, such as layered limestones and dolomites with  
130 cherts (Compagnoni et al., 2005; Corò et al., 2015). Because of its morphological  
131 characteristics, the study area is affected by slope instability, which overlay an area of 165 km<sup>2</sup>  
132 corresponding to 6% of the province (Baglioni et al., 2006). Most of the landslides are located  
133 in the NW (Upper basin of Cordevole River) and SE (Alpago district) sectors of the province  
134 (Figure 1). The dominant landslide types are slides (47%), rapid flows (20%), slow flows  
135 (12%), and shallow soil slips (7%) (Iadanza et al., 2021). The climate of the province of Belluno  
136 is continental. The mean annual temperature recorded in the period 1961–1990 is 7°C and the  
137 mean precipitation is 1284 mm/year (Desiato et al., 2005) with two peaks distributed in spring  
138 and autumn. In the last 27 years, temperature and rainfall intensity in the study area have  
139 increased due to climatic changes leading to more frequent meteorological conditions  
140 (ARPAV, 2021 ).

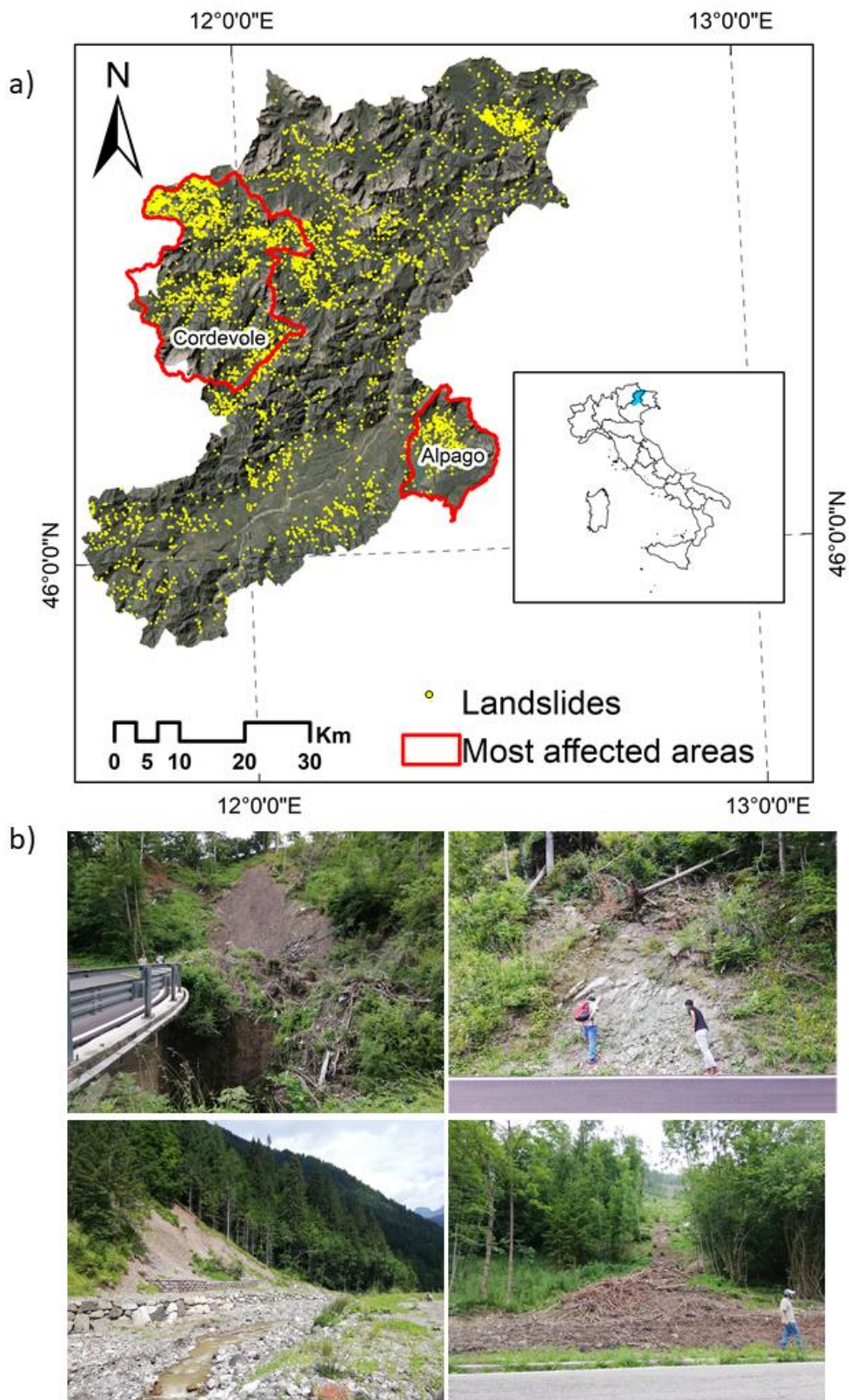


Figure 1: a) Location of the study area and landslides collected by IFFI (Inventory of Landslide Phenomena in Italy) project b) field photographs after the VAIA event.



## 2.2 Landslide inventory data

The inventory of landslide phenomena in Italy (IFFI) conducted by the Italian Institute for Environmental Protection and Research (ISPRA) and the Regions and Autonomous Provinces was used in this study (Trigila et al., 2010). The IFFI Project was financed in 1997. Since 2005, the catalogue is available online and consists of point features indicating the scarp of the landslides and polygon features delineating the instabilities. The archive stores the main attributes of the landslides, such as morphometry, type of movement, rate, involved material, induced damages and mitigation measures. The inventory currently holds 620,808 landslides collected from historical documents, field surveys and aerial photointerpretation, covering an area of 23,700 km<sup>2</sup>, which corresponds to the 7.9% of the Italian territory (Trigila and Iadanza, 2018). In the Belluno province, the IFFI inventory consists of 5934 points of landslides occurred before 2006 (Baglioni et al., 2006).

## 2.3 Landslide conditioning factors

Based on the regional environmental characteristics of the study area and the scientific literature, fourteen landslide conditioning factors were selected, including: (i) topographical factors such as elevation, slope angle, slope aspect, topographical wetness index (TWI), topographical position index (TPI), topographical roughness index (TRI), profile curvature, and plan curvature; (ii) hydrological factors (i.e., distance to drainage, Mean monthly rainfall); geological factors (lithology); (iii) anthropogenic factors (distance to roads); and (iv) environmental factors like Normalized Difference Vegetation Index (NDVI) and landcover (see figure 2). A freely accessible digital elevation model (DEM) with a spatial resolution of 25 metres and was downloaded from the Veneto Region cartographic portal (<https://idt2.regione.veneto.it>), was used to derive the topographic layers. Refer to table 1 for a detailed description of the conditioning factors. Land cover, lithology maps, road network and



drainage maps were downloaded from the same portal. Rainfall data was downloaded from the Regional Agency for the Environmental Prevention and Protection of Veneto (ARPAV: <https://www.arpa.veneto.it/>) web site. We resampled the conditioning factor maps to 25 meter pixels in order to do the analysis.

Table 1: Description of the conditioning factors for landslide occurrences.

Sl No.	Conditioning Factor	Data Range	Description/Justification
1	Elevation	42 m to 3325 m	The geomorphological and geological processes are affected by elevation (Raja et al., 2017). It has an impact on topographic characteristics, which contribute to spatial differences in many landform processes, as well as the distribution of vegetation. <u>Elevation largely influences climate, including the amount, intensity and distribution of rainfall.</u>
2	Slope	Flat areas to very high slopes till 86°	Slope is a derivative of the DEM which can cause failure of slope (Pham et al., 2018). Landforms having a higher angle of slope are usually more susceptible to collapse, which is closely correlated to landslides.
3	Aspect	North (0 degrees) to North (360 degrees)	Aspect has a correlation with other geo-environmental factors <u>and</u> is a crucial factor <u>that describes the slope direction</u> (Dahal et al., 2008). The slope direction, to a degree, dictates the frequency of landslides <u>(Ruff and Czurda 2008).</u>

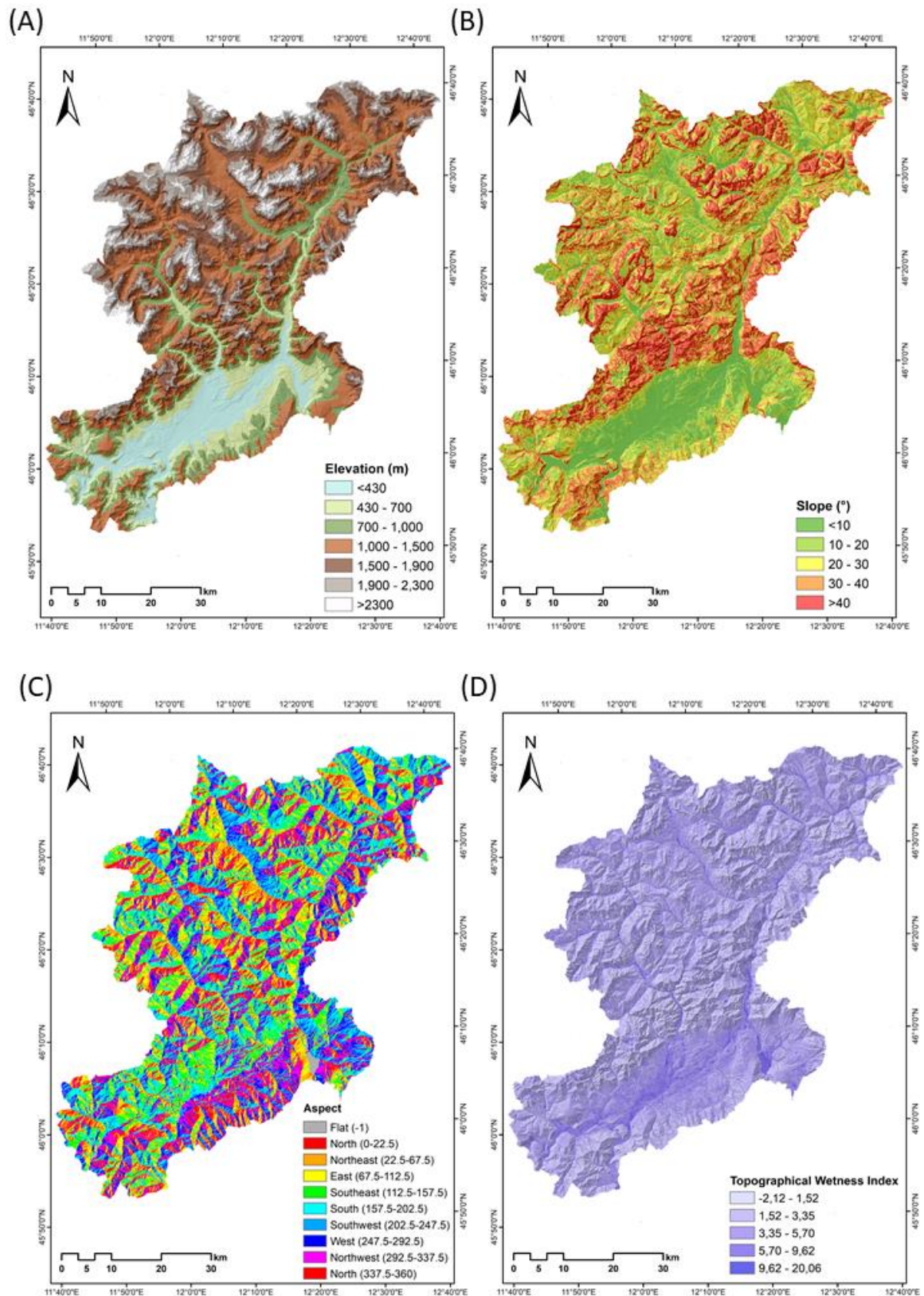
4	Topographic wetness index	-2.12 to 20.06	The influence of topography on the location and amount of saturated runoff source areas is an essential conditioning factor (Pourghasemi et al., 2012). TWI <u>estimates</u> the amount of accumulated water and distribution of soil moisture at a location. Higher TWI values can relate to higher chances of landslide occurrence.
5	Topographic Position Index	-1143.68 to 243.84	The topographic position index (TPI) shows the difference between the elevation of a point and its surrounding. Lower values represent the plausibility of features lower than the surrounding, thus possibly relating to higher odds of landslide occurrence.
6	Topographic Roughness Index	0 to 1077.30	Topographic Roughness Index (TRI) calculates the difference in elevation between adjacent pixels in a DEM which depicts the terrain fluctuation (Riley et al., 1999). As the slope of a landscape <u>changes in space</u> , the TRI decreases, relating to slope movement.
7	Profile Curvature	Concave <u>(-197)</u> Flat <u>(0)</u> Convex <u>(304)</u>	The driving and resisting forces within a landslide in the slope direction are affected by profile curvature.
8	Plan Curvature	Concave <u>(-370)</u> Flat <u>(0)</u>	The direction of landslide movement is controlled by the plan curvature, which regulates

		Convex <a href="#">(95)</a>	the convergence or divergence of landslide material (Dury, 1972; Meten et al., 2015).
9	Drainage	0 to 400	Drainage transports water, which induces material saturation, culminating in landslides in valleys. (Shahabi and Hashim, 2015).
10	<a href="#">Mean</a> <a href="#">monthly</a> Rainfall	84 to 1198.05 (mm/month)	Rainfall characteristics shift by climatic conditions and geographical characteristics, resulting in significant temporal and geographical variations in rainfall quantity and intensity. This can lead to the triggering of landslides across large areas but also for specific smaller areas.
11	Lithology	Volcanites, Pre-Permian, metamorphic, sequence Morainic, Gravels, <a href="#">Mix of</a> <a href="#">alluvial</a> <a href="#">deposits,</a> <a href="#">Conglomerate,</a> <a href="#">Limestone ad</a> <a href="#">dolomitic</a> <a href="#">limestone,</a> <a href="#">Calcareous</a>	The geological strength indices, failure susceptibility, and permeability of lithological units differ where changes in the stress-strain behaviour of the rock strata can be caused by lithological unit variation. Slope failure typically occurs on a slope with low shear strength <a href="#">Segoni et al., 2020</a> .

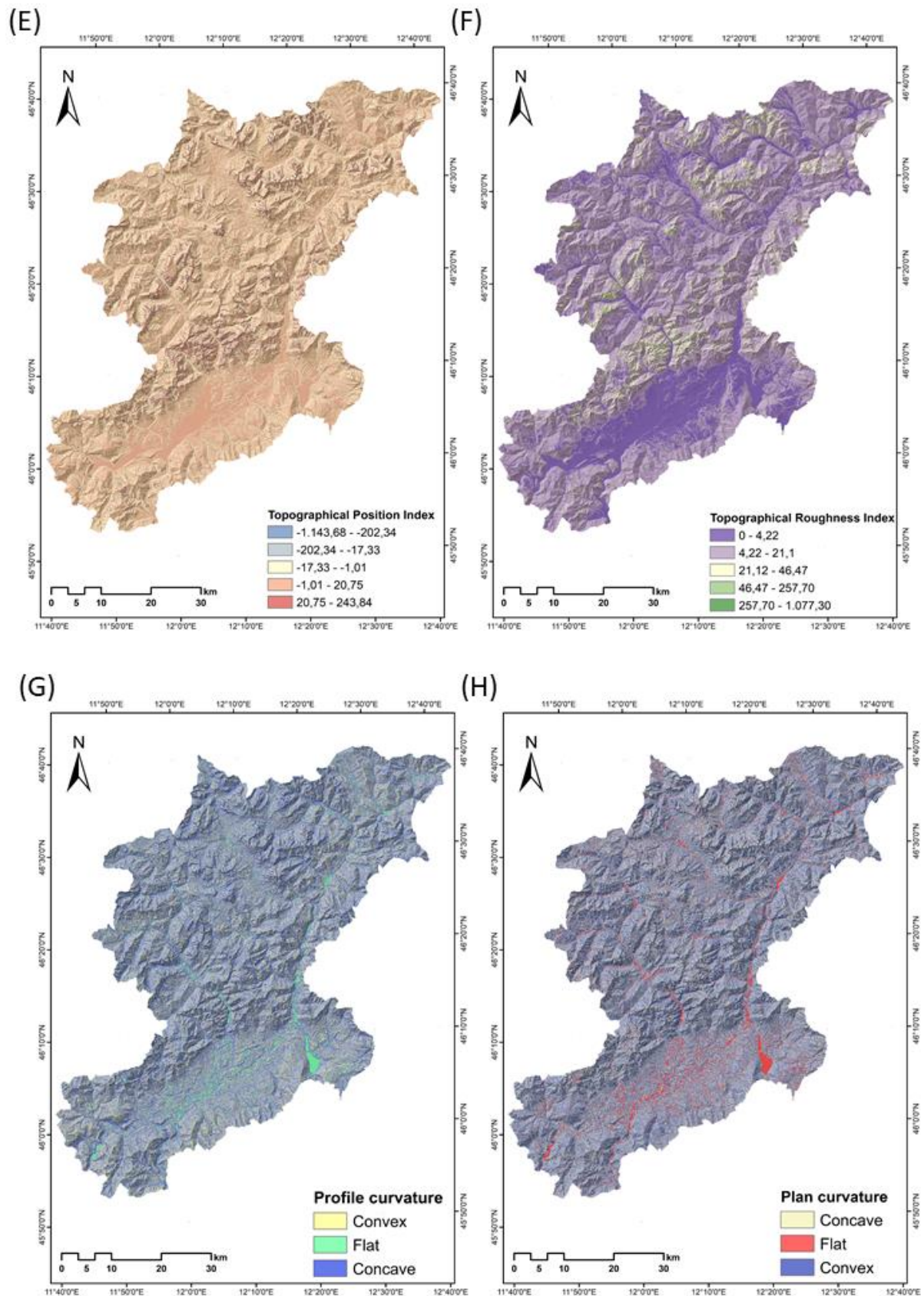
		<u>shales, Shales</u> <u>and gypsums,</u> <u>Alternation of</u> <u>marl and</u> <u>sandstones,</u> <u>water body.</u>	
12	Distance to Roads	0 to 200	A crucial manmade element impacting the occurrence of landslides is roads because of road clear-cutting and construction activities (Dunning et al., 2009).
13	Landcover	<u>Urban cover,</u> <u>Rock, Arable,</u> <u>Permanent</u> <u>cultivation,</u> <u>Forest,</u> <u>Grassland,</u> <u>Shrubland,</u> <u>Sparse</u> <u>vegetation,</u> <u>Water body</u>	Because land cover may influence the hydrological functioning of slopes, rainfall partitioning, infiltration properties, and runoff, as well as the soil shear strength, different land cover types may affect slope stability.
14	NDVI	-0.66 to 0.66	NDVI is important in realizing the amount of vegetation cover which can be interpreted to understand the strength of the slope and the landslide occurrences. The NDVI reflects the

			inhibitory effect of landslide occurrence (Huang et al., 2020).
--	--	--	---

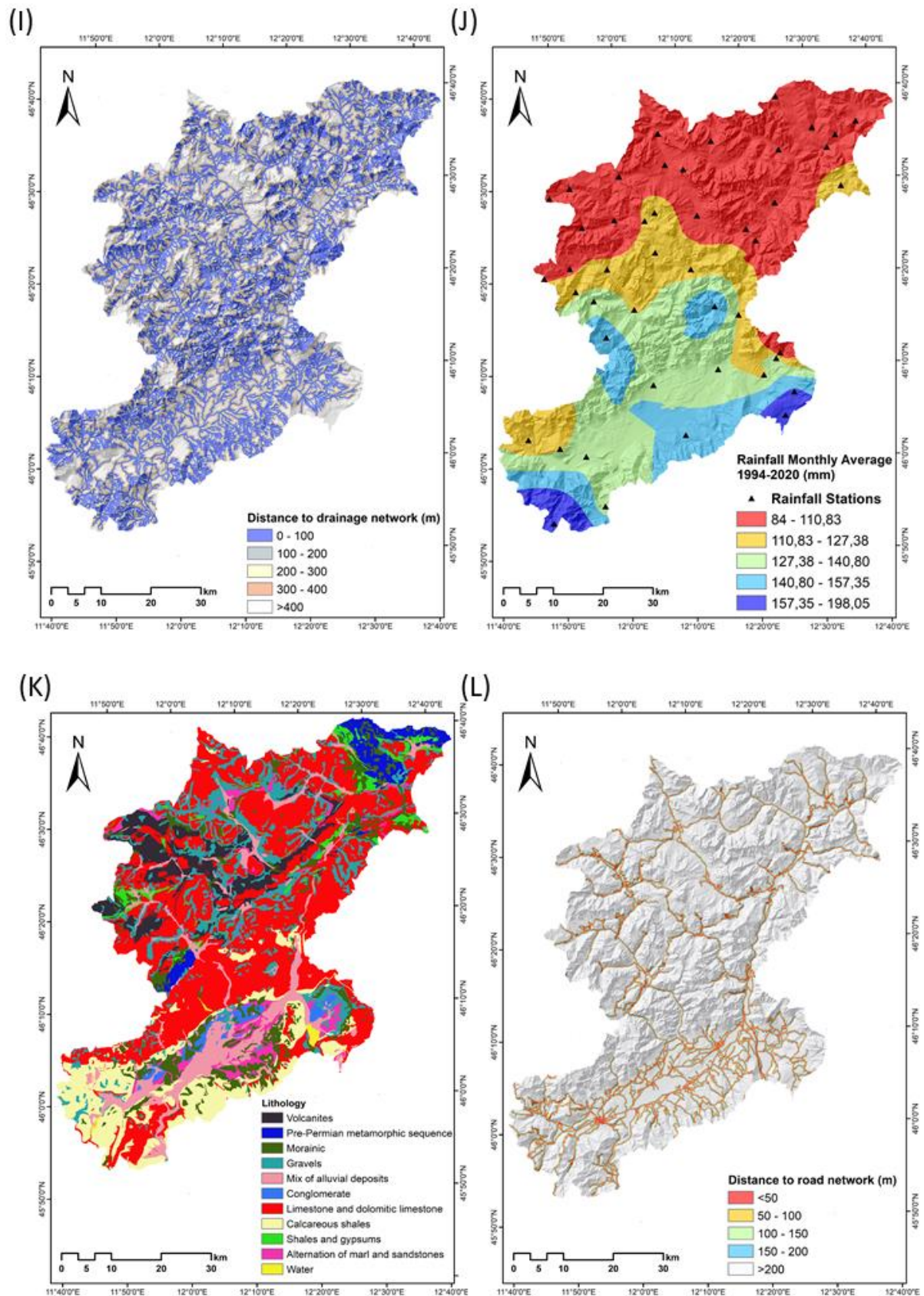
175











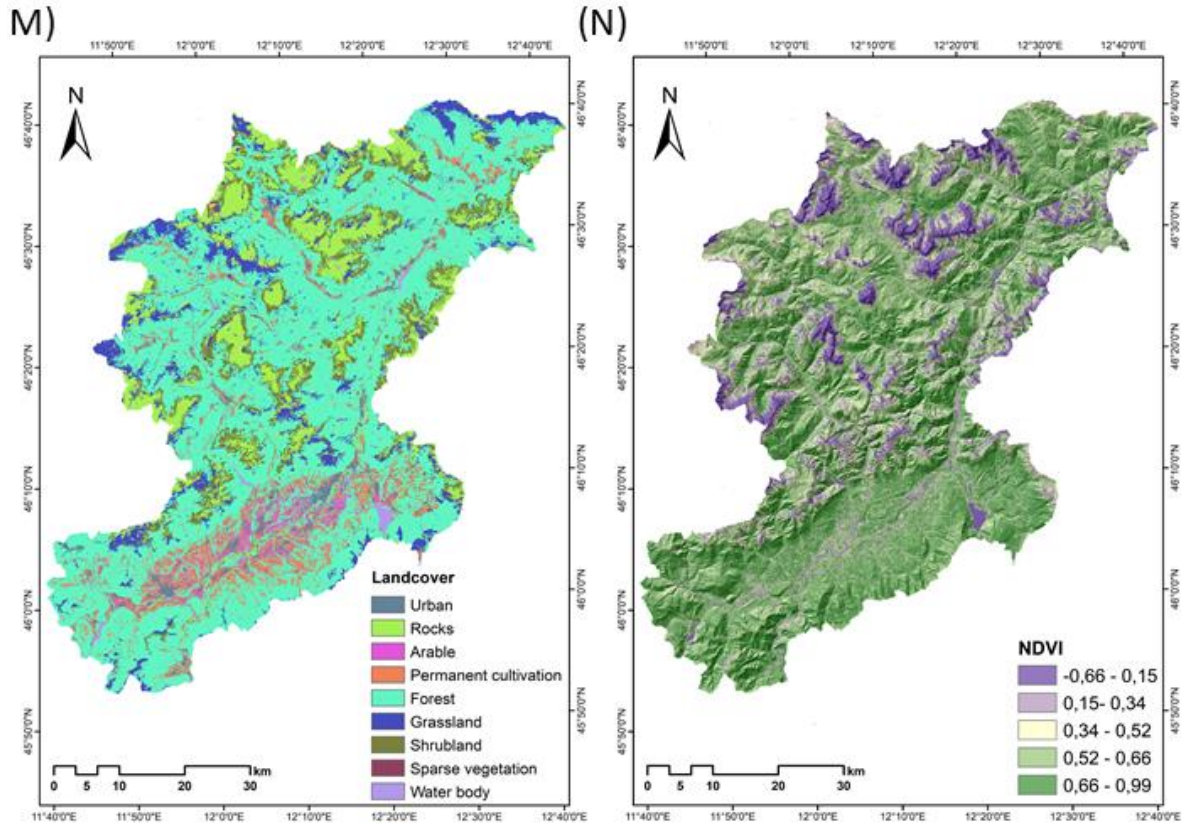


Figure 2: Maps of the conditioning factors used in this study: (A) Elevation, (B) Slope, (C) Aspect, (D) Topographical wetness index, (E) Topographical position index, (F) Topographical roughness index, (G) Profile curvature, (H) Plane curvature, (I) Distance to drainage networks, (J) Rainfall monthly average (1994-2020) mm, (K) Lithology, (L) Distance to road network (M) Landcover, (N) NDVI

### 3. Methodology

We propose an approach that helps assess importance of the conditioning factors, which can help improve the susceptibility results by removing the less "important" factors throughout the statistical and ML models. As stated previously, the study attempts the application of sensitivity analysis to understand relative importance of the conditioning factors as a preliminary step towards improving the landslide susceptibility prediction capability. In this study, the LSM

193 was obtained by the combination between IFFI landslide inventory and the conditioning factors  
194 through statistical methods such as [Evidence Belief Function \(EBF\)](#) and ML models, i.e.  
195 Random Forest and XG-Boost  
196 (Figure 3). The successive sub-sections address the definitions of the statistical and ML models  
197 for LSM.

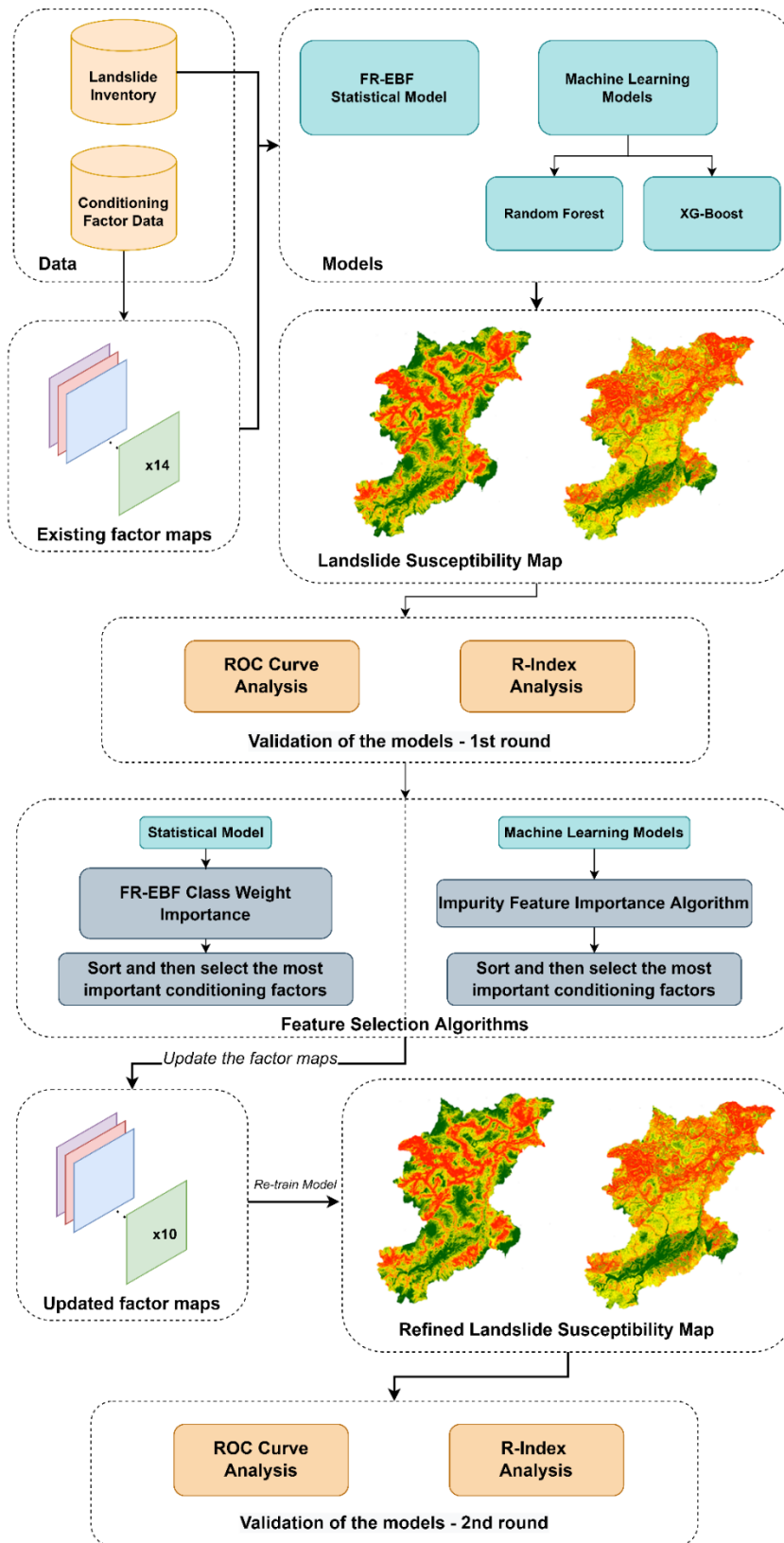


Figure 3: Overview of the conceptual workflow of methodology for landslide susceptibility assessment.

### 3.1 Statistical approach

#### 3.1.1 Ensemble Frequency Ratio - Evidence Belief Function

In landslide susceptibility studies, the frequency ratio (FR) model is often applied. This is an evaluation method which calculates the likelihood of landslide occurrence and non-occurrence for each conditioning factor. (Lee, 2013; Mondal and Maiti, 2013; Shahabi et al., 2014). For each landslide conditioning factor, the FR is a probabilistic model based on observed correlations between landslide distribution and related parameters (Lea Tien Tay 2014). The model depicts the relationship between spatial locations and the factors that determine the occurrence of landslides in a specific area. Spatial phenomenon and factor classes correlation can be found through FR and is very helpful for geospatial analysis (Mahalingam et al. 2016; Meena et al. 2019b). Figure 3 gives an overview of the methodology employed in this study. FR weights can be computed using the ratios of landslide inventory points of all classes within each factor. The landslide inventory points are then overlaid with the conditioning factors to obtain the area ratio for each factor class to the total area. The FR weights are then obtained by dividing the landslide occurrence ratio in a class by the area in that class (Demir et al. 2012).

Using the Eq. 1, the Landslide Susceptibility Index (LSI) was computed by summing the values of each factor ratio (Lee, 2013):

$$LSI = \sum FR \text{ (Eq.1)}$$

$$LSI = (DEM * wi) + (slope * wi) + (aspect * wi) + (Topographic Wetness Index * wi) + (Topographic Roughness Index * wi) + (Topographic Position Index * wi) + (Distance to road * wi) + (Distance to drainage * wi) + (Land Cover * wi) + (Lithology * wi) + (NDVI * wi) + (Rainfall * wi) + (Profile Curvature * wi) + (Plain Curvature * wi)$$



Where LSI is the landslide susceptibility index, FR is the frequency ratio of every factor type or class, and  $w_i$  is the weight of each conditioning factor. The higher the LSI value, the higher the susceptibility to landslides.

We integrated the LSI results with [EBF](#) derived predictor values. The EBF uses the conditioning factors defined by FR as the input data. Eq. (2) was applied to the rating of every spatial factor.

$$PR = \frac{SA_{max} - SA_{min}}{SA_{max} - SA_{min}} min \text{ (Eq.2)}$$

where SA is the indicator of Spatial Association between spatial factors and landslides, whereas PR is the Prediction Rate. The lowest absolute difference of all factors is divided by the computed absolute difference between the maximum and the least SA values (Table 2). Pairwise comparison of the PR values of the slope failure predictors yielded the pairwise rating matrix of the predictor rating. We used PR values for assigning weights of the factors for susceptibility analysis.

## 3.2 Machine learning models

### 3.2.1 Random Forest model

Random Forest (RF) is based on the concept of the "wisdom of crowds" where multiple decision trees, introduced by (Breiman, 2001), has been utilized in a number of remote sensing research for a variety of applications (Melville et al., 2018). RF creates many deep decision trees using the training data and it can overcome the overfitting problem mostly resulting from complex datasets better than other decision trees. Each RF decision tree gives a prediction, which is then weighted according to the value created from votes from each tree leading to generation of the susceptibility map (see figure 4). Since the RF has shown an impressive performance for classification purposes, it is regarded as one of the most efficient non-

parametric ensembles models (Chen et al., 2017). Based on the advantages listed above, the RF model is used to assess landslide susceptibility. Landslide inventories along with the conditioning factors are divided into training and testing data as seen in figure 4. Using the bagging technique, the training data is divided into training subsets, generally about one-third of the total training samples. A decision tree is created for each subset based on the training subset defined in the first stage and accordingly, votes as implemented that outputs the landslide susceptibility.

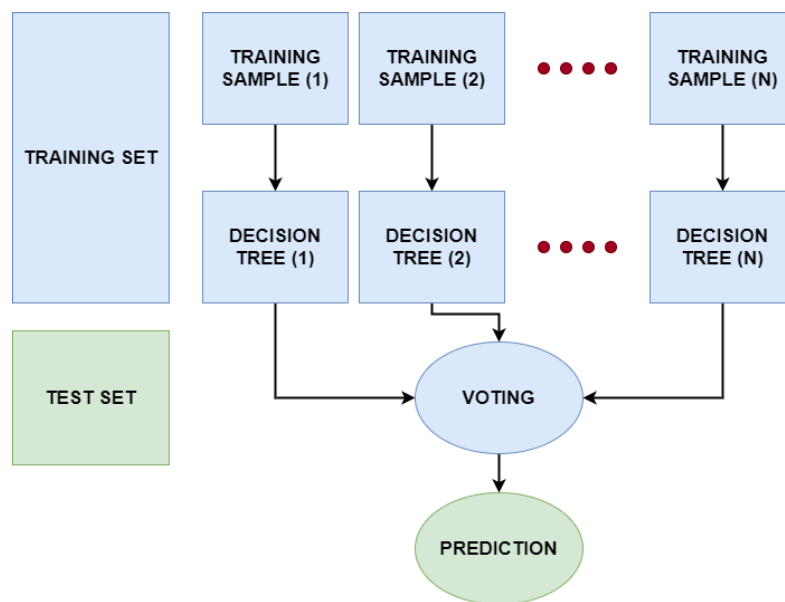


Figure 4: Conceptual diagram of the Random Forest model.

### 3.2.2 XG-Boost model

Extreme gradient boosting or commonly known as the XG-Boost ML model is an optimized gradient boosting algorithm that is designed for optimum speed and performance and boosting ensembles are used to generate a prediction model (Sahin, 2020). The core idea of a boosting algorithm is to combine the weaker learners to improve accuracy (Can et al., 2021), meaning that different models with lower susceptibility accuracies are “boosted” by combining them to achieve an ensembled higher susceptibility accuracy. The model is known for its fast-training



speed for classification tasks. In the study, we use training parameters to adjust the XG-Boost algorithm like learning rate, subsample ratio, maximum depth of the tree and others. It uses boosting techniques to reduce overfitting problems to improve accuracy results (figure 5). The training data is divided into subsets which are then trained using a tree ensemble model. This means that every weight derived from each model training of landslide instances in the area are added and then predicted on the test set with the average landslide susceptibility scores of the ensemble models.

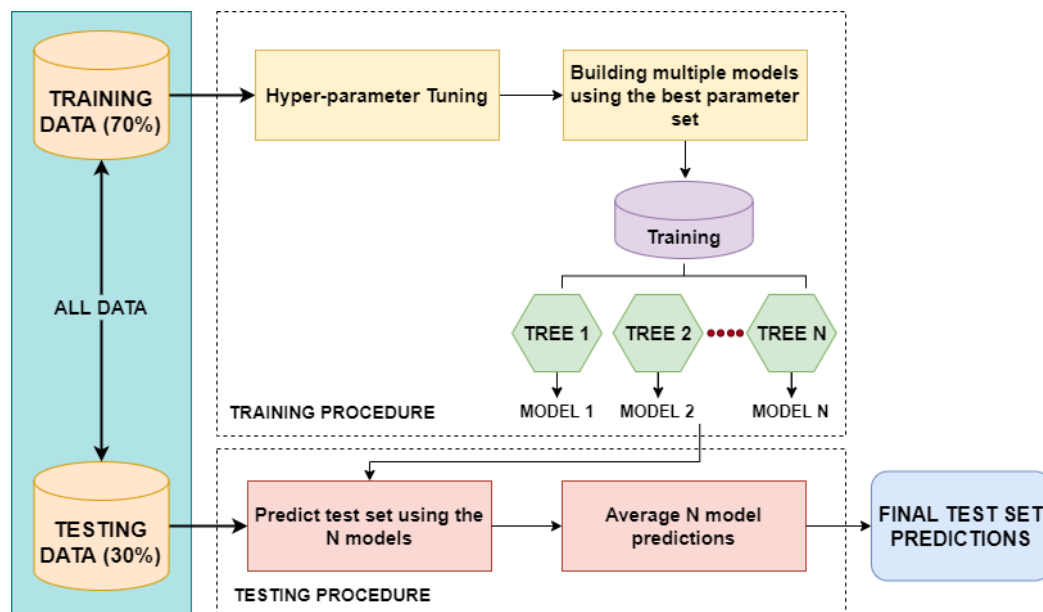


Figure 5: Training and testing procedure of the XG-Boost model.

### 3.3 Feature selection algorithms

The goal of feature selection is to remove the least important conditioning factors in order to increase the generalisability in landslide prediction. This selection help eliminates the irrelevant (less important) conditioning factors to obtain optimal prediction accuracy (Micheletti et al., 2014). For the statistical model, we used class weights obtained from frequency ratio and used them as input for generating predictor rate from FR-EBF model which

gives the final weights of the conditioning factors. So, we used the predictor rate weights to select the suitable features.

In terms of the feature importance for selecting the right set factors for both RF and XG-Boost, we use the in-built impurity feature importance algorithm which is performed on the training set (refer to feature selection in figure 3). Based on the results of the feature selection algorithms for the conditioning factors for each model, the most important factors will be selected to investigate the improvement of model performance. With this, we can understand which of the conditioning factors played the most important roles in giving the highest accuracy for each ML model.

## 4. Results

### 4.1 Statistical model

The class weights were derived from data driven FR model and the final weights of the factors were derived by using predictor rate from evidence belief function given in Table 2. The class and factor weights were calculated using equations 1 and 2. The final weights of landslide conditioning factors were calculated using an ensemble of FR-EBF, and then utilised to create the final LSM. Because there is no common approach for identifying landslide susceptibility classes in the final LSM, we normalised the findings to 0 to 100 for uniformity and comparability. Using a [quantile](#) classification, which separates the values into groups with random number of values, the resultant LSM was classified into five classes: very low, low, moderate, high, and very high, as shown in figure 7 (Chung and Fabbri, 2003). This method of classification gives a better distribution of values in each class than common approaches such as natural breaks, which can result in certain classes having limited or excessive data.

In terms of the feature importance that we observe in figure 6 and Table 2 (normalized weights), based on the trial-and-error approach, factors (or features) under the threshold of 0.3 were discarded as they did not make much of a difference in terms of predicting landslide

occurrences in the study area. Therefore, five conditioning factors having coefficient values lower than 0.30 were dropped and overall, the area under the curve (AUC) accuracy still remained similar to the original accuracy with the 14 factors.

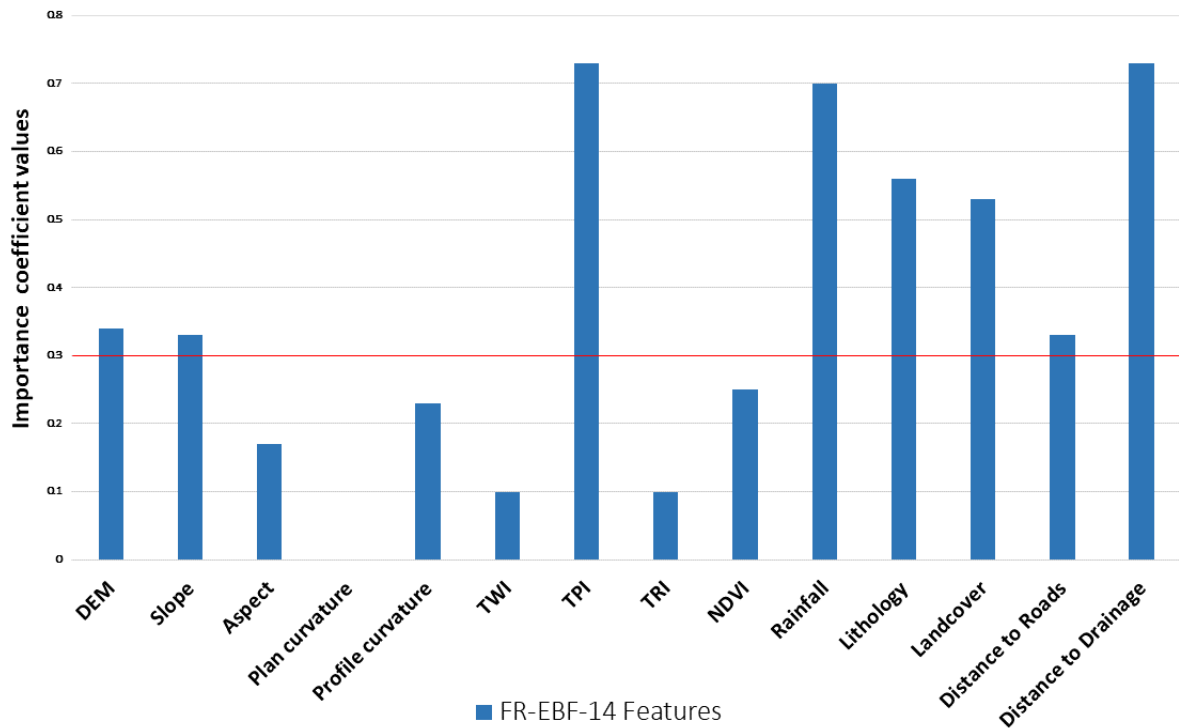


Figure 6: Feature importance of the statistical model (Horizontal red line shows 0.3 as the cut-off value).

Table 2: Frequency ratio values for spatial factors class weighting and EBF coefficients for predictor rates (PR) based on degrees of spatial associations.

Factors and classes	Bel	Min	Max	[Max-Min]	Predictor Rate	FR Weights	Normalized weights
Elevation		0.07	0.24	0.17	0.73		
<430	0.07					0.50	0.06
430 - 700	0.15					1.13	0.20
700 - 1000	0.13					0.96	0.19

1000 - 1500	0.12				0.86	0.15
1500 - 1900	0.11				0.81	0.12
1900 - 2300	0.24				1.72	0.17
>2300	0.18				1.31	0.12
Profile		0.00	0.53	0.53	2.30	
Curvature						
Concave	0.53				1.05	0.40
Flat	0.00				0.00	0.30
Convex	0.47				0.95	0.30
Plan		0.00	0.52	0.52	2.26	
Curvature						
Concave	0.52				1.03	0.35
Flat	0.00				0.00	0.33
Convex	0.48				0.97	0.32
Slope		0.14	0.25	0.11	0.48	
<10	0.14				0.70	0.14
10 - 20	0.23				1.11	0.22
20 - 30	0.25				1.25	0.27
30 - 40	0.20				0.99	0.20
>40	0.17				0.86	0.17
Distance from		0.02	0.36	0.34	1.49	
drainage						
0 - 100	0.36				1.15	0.28
100 - 200	0.30				0.97	0.19
200 - 300	0.23				0.74	0.12
300 - 400	0.10				0.31	0.07
>400	0.02				0.06	0.34
Distance from		0.08	0.24	0.15	0.67	
roads						
0 - 50	0.36				1.15	0.27

50 - 100	0.30				0.97	0.19
100 - 150	0.23				0.74	0.17
150 - 200	0.10				0.31	0.16
>200	0.02				0.06	0.13
Landcover		0.01	0.24	0.23	2.98	
Urban	0.17				1.48	0.17
Rocks	0.10				0.90	0.09
Arable	0.01				0.07	0.01
Permanent	0.10				0.92	0.13
cultivation						
Forest	0.11				0.95	0.11
Grassland	0.24				2.11	0.14
Shrubland	0.04				0.37	0.04
Sparse	0.12				1.08	0.21
vegetation						
Water body	0.12				1.05	0.09
TWI		0.17	0.25	0.08	1.00	
-2.12 - 1.52	0.19				1.01	0.20
1.52 - 3.35	0.20				1.04	0.20
3.35 - 5.70	0.18				0.92	0.18
5.70 - 9.62	0.17				0.90	0.18
9.62 - 20.06	0.25				1.30	0.24
TPI		0.00	0.31	0.31	1.35	
-1143.68 - -	0.00				0.00	0.00
202.34						
-202.34 - -	0.18				0.74	0.21
17.33						
-17.33 - -1.01	0.26				1.06	0.27
-1.01 - 20.75	0.24				0.98	0.26
20.75 - 243.84	0.31				1.24	0.27

TRI		0.00	0.34	0.34	1.47		
0 - 4.22	0.22					0.73	0.23
4.22 - 21.1	0.34					1.11	0.35
21.12 - 46.47	0.25					0.82	0.22
46.47 - 257.70	0.20					0.65	0.20
257.70 - 1077.30	0.00					0.00	0.00
Rainfall intensity		0.00	0.81	0.81	3.54		
84 - 110.83	0.81					11.29	0.32
110.83 - 127.38	0.08					1.15	0.27
127.38 - 140.80	0.05					0.70	0.15
140.80 - 157.35	0.06					0.81	0.19
157.35 - 198.05	0.00					0.00	0.06
NDVI		0.14	0.25	0.11	0.48		
-0.66 - 0.15	0.14					0.70	0.13
0.15 - 0.34	0.22					1.13	0.21
0.34 - 0.52	0.25					1.26	0.25
0.52 - 0.66	0.21					1.07	0.21
0.66 - 0.99	0.18					0.89	0.20
Aspect		0.05	0.15	0.09	0.41		
Flat (-1)	0.11					1.02	0.10
North (0-22.5)	0.08					0.75	0.07
Northeast (22.5-67.5)	0.09					0.84	0.09

East (67.5-112.5)	0.11				1.08	0.11
Southeast (112.5-157.5)	0.14				1.31	0.14
South (157.5-202.5)	0.15				1.40	0.14
Southwest (202.5-247.5)	0.14				1.33	0.14
West (247.5-292.5)	0.08				0.76	0.09
Northwest (292.5-337.5)	0.05				0.50	0.07
North (337.5-360)	0.06				0.58	0.06
<hr/>						
Lithology		0.04	0.26	0.22	2.84	
Volcanites	0.26				3.45	0.16
Pre-Permian metamorphic sequence	0.11				1.50	0.11
Morainic	0.06				0.85	0.15
Gravels	0.04				0.52	0.04
Mix of alluvial deposits	0.05				0.70	0.03
Conglomerates	0.21				2.84	0.21
Limestone and dolomitic limestone	0.13				1.76	0.16



Calcareous shales	0.08		1.04	0.08
Shales and gypsums	0.06		0.76	0.07
Alternation of marls and sandstones	0.07		0.91	0.06
Water body	0.22		2.97	0.00

322

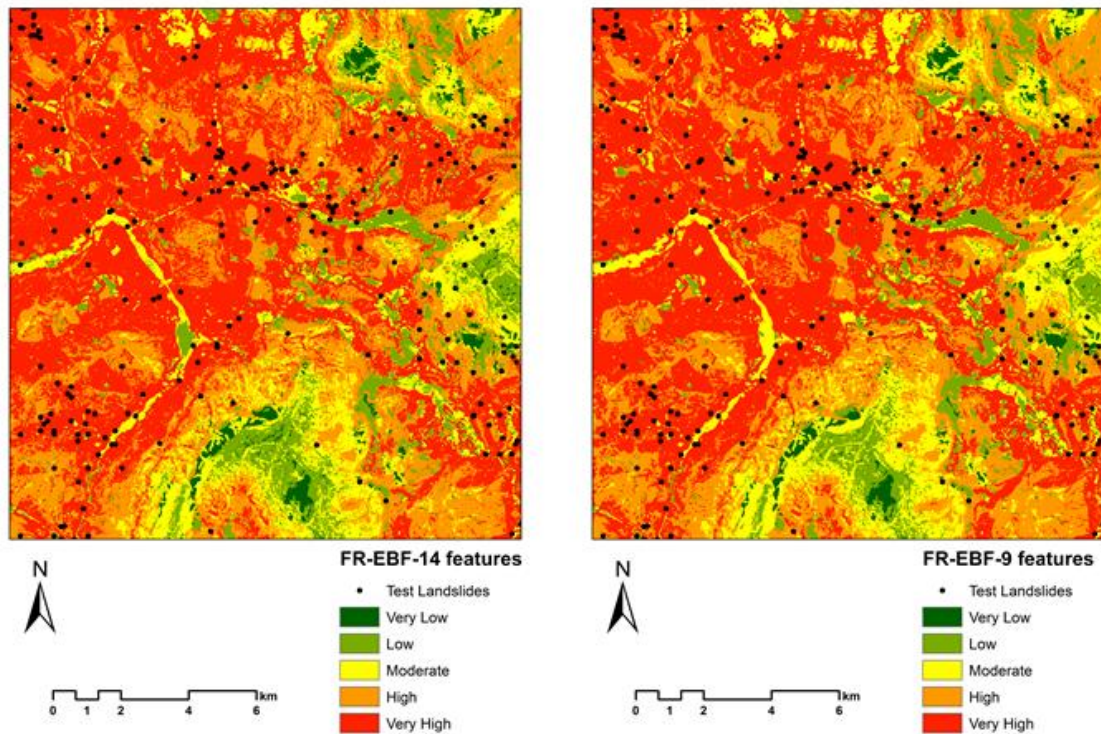
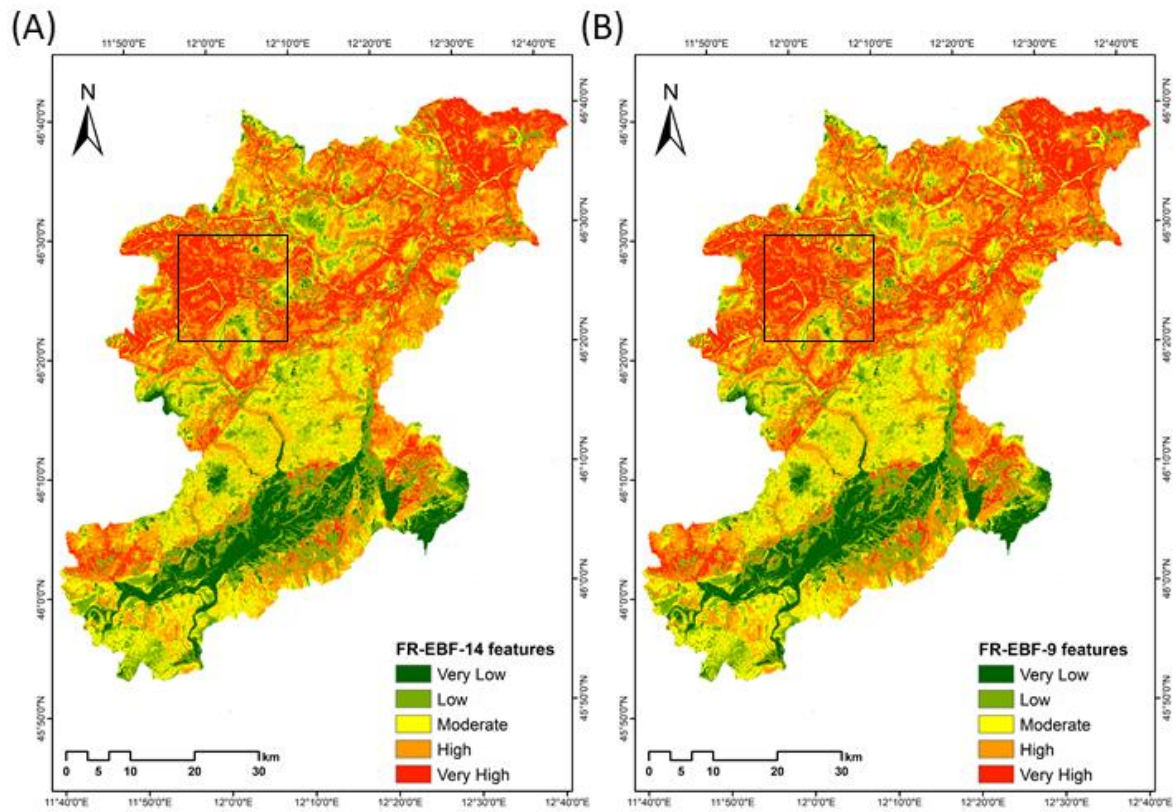


Figure 7: Landslide susceptibility maps derived using the ensemble of FR-EBF approaches for (A) 14 landslide features and (B) 9 landslide features (Black square represents the enlarged area).

#### 4.2 Machine learning models

The LSM was generated based on the conditioning factor data, where the model learnt the information from the feature maps, which helped identify areas of susceptibility. The final results of the ML models in generating the LSM are given in Table 3. We observe that the AUC scores of RF are not much apart from the XG-Boost model, indicating similar predictive skills of both the models. Visually the results show more susceptible areas near the landslide features (figures 8 and 9).

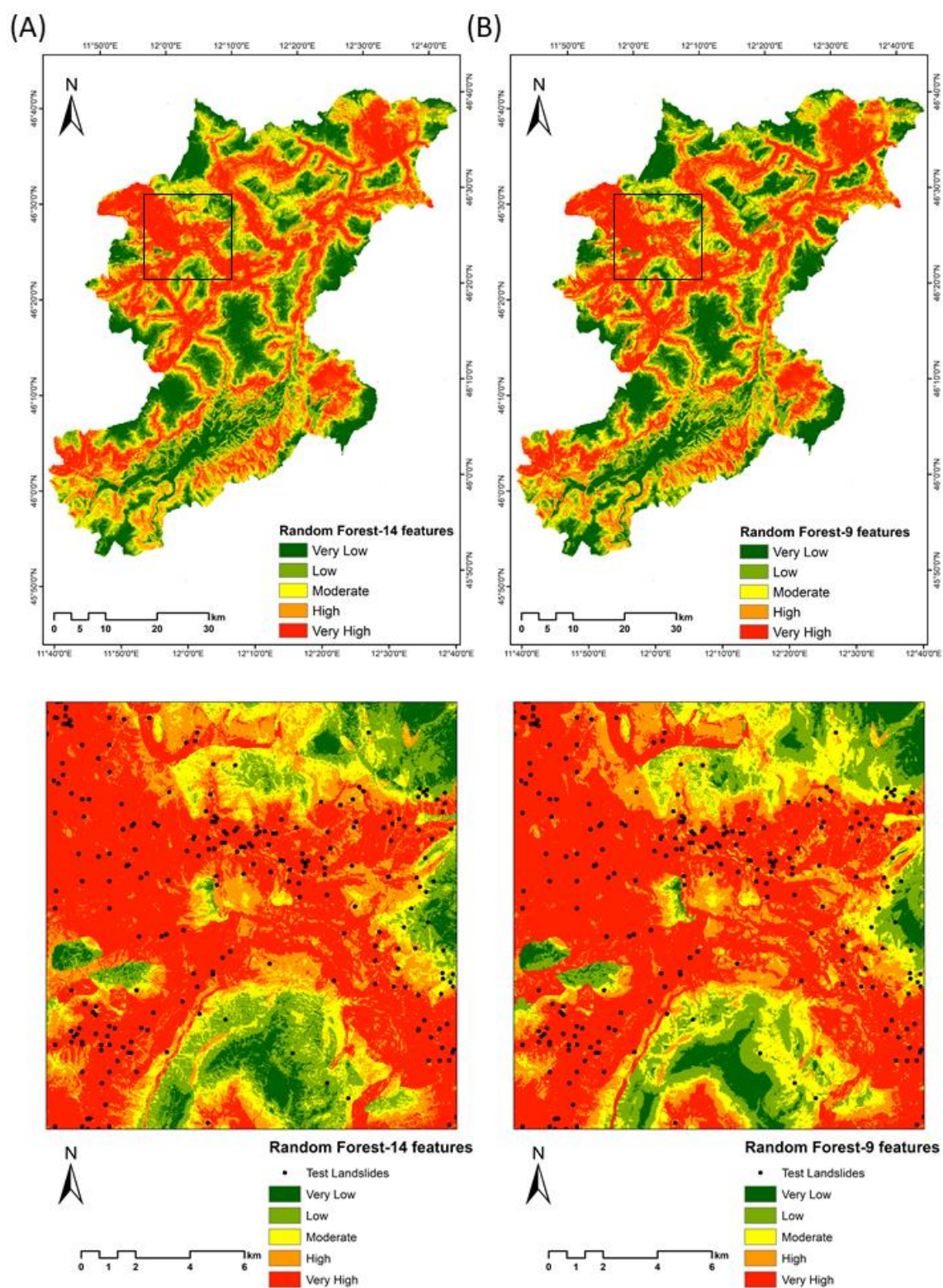
The model performance in terms of the accuracy of AUC is relatively similar to the results after eliminating the lower degree of feature importance for both RF and XG-Boost. As discussed previously in section 3.3, the feature importance for the ML models is carried out using the impurity feature importance algorithm that enables to assess the relative relevance of the conditioning factors in the optimal prediction of the landslides in terms of accuracy. As seen in figure 10, the factors of Landcover, Profile Curvature, Plan Curvature, TWI and TPI have the lowest values for the RF model. We examined various values as a cut-off for choosing the "important" conditioning factors and after much trial-and-error, a value of 0.03 was chosen as the threshold. Any factors above this value were considered as "important" factors for landslide susceptibility, hence, in figure 8, we see that the five factors mentioned above are removed and giving us 0.906 AUC as accuracy, which is better in AUC accuracy without removing the five factors (0.902 AUC as seen in Table 3).

Similarly, the same was repeated for the XG-Boost ML model and referring to Table 3, and despite removing the lower valued conditioning factors of Profile Curvature, TPI, and Plan Curvature, the AUC accuracy score was similar (Table 3). We observe that Slope and Distance

to Roads had a much bigger impact on the RF mode than the XG-Boost model. On the other hand, Lithology played a bigger role in estimating landslide occurrences in the XG-Boost model. These observations indicate interesting results which will be discussed further in the discussion section.

Table 3: Overall table with AUC results for landslide susceptibility of Belluno.

No.	Model	AUC
1	FR-EBF 14 features	0.836
2	FR-EBF 9 features	0.834
3	RF 14 features	0.902
4	RF 9 features	0.906
5	XG-Boost 14 features	0.910
6	XG-Boost 10 features	0.907



358

359



360 Figure 8: LSMs derived using the Random Forest approach for (A) 14 landslide features and  
361 (B) 9 landslide features (Black square represents the enlarged area).

362

363

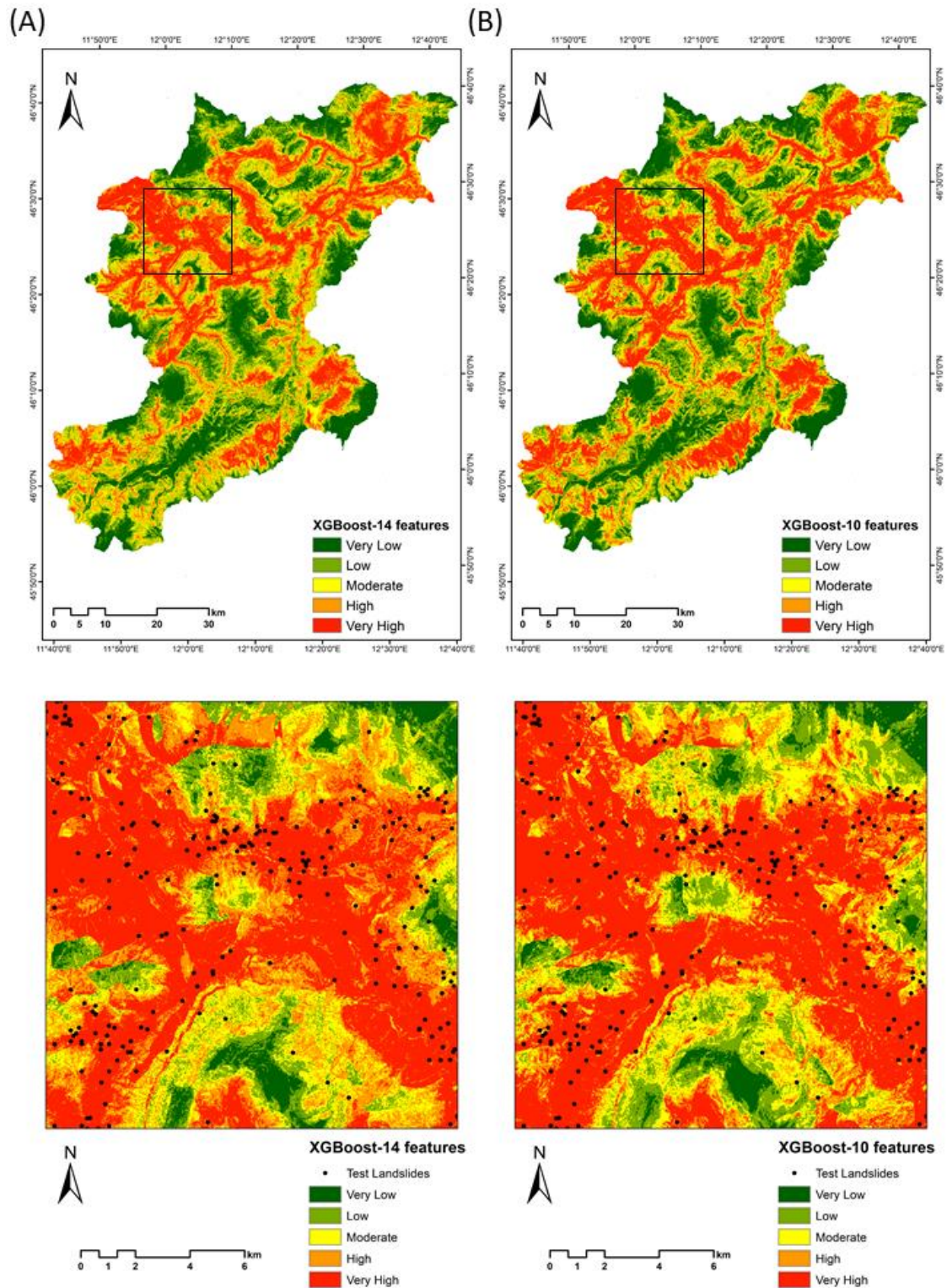


Figure 9: LSMs derived using the XG-Boost approach for (A) 14 landslide features and (B) 9 landslide features (Black square represents the enlarged area).



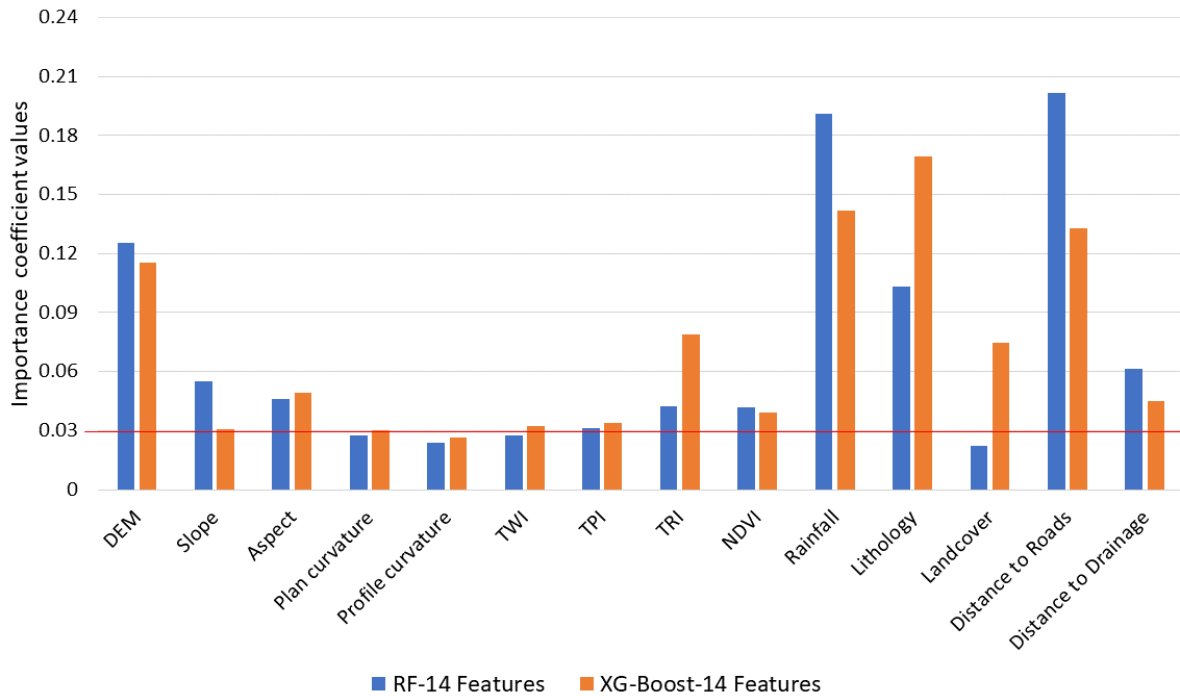


Figure 10: Feature importance of the RF and XG-Boost models (Horizontal red line shows 0.3 as the cut-off value).

## 5. Accuracy Assessment

Accuracy assessment is crucial in producing quality LSMs for natural hazards where the information presented in the map is beneficial for planners (Goetz et al., 2015). A number of accuracy assessment approaches may be used to assess the quality of the LSMs. We compare the landslide inventory data to the resultant maps derived using the ensemble of FR-EBF, machine learning RF and XG-Boost models. The efficiency of any model for LSM is calculated by comparing the inventory data to the produced maps. This reflects if the models in use can accurately forecast which areas are susceptible to landslides (Pourghasemi et al., 2018). The findings from the total landslide input events were tested using 30% of the landslide occurrences. Testing for this study was done using the Receiver Operating Characteristics (ROC) and the Relative Landslide Density (R-Index) approaches.

## 5.1 Receiver Operating Characteristics (ROC)

The test dataset was used to corroborate the six resultant LSMs from statistical and machine learning using the receiver operating characteristics (ROC) approach. The ROC approach shows how to evaluate the true positive rate (TPR) and false positive rate (FPR) in the LSMs (Ghorbanzadeh et al., 2018; Linden, 2006). TPRs are pixels that are correctly labeled as high susceptibility in the landslide validation data, whereas FPRs are pixels that are incorrectly labeled. ROC curves are created using TPRs versus FPRs. The accuracy of the generated LSMs is determined by the AUC. The AUC shows whether there were more correctly labeled pixels than incorrectly labeled pixels. Greater AUC values suggest a more accurate susceptibility map, and vice versa. The susceptibility map is meaningful if the AUC values are close to unity or one. A map with a value of 0.5 is considered insignificant since it was created by chance. (Baird, 2013).

Figure 11 shows the accuracy values obtained using the ROC technique for the statistical approaches of FR-EBF and machine learning approaches of RF and XG-Boost. XG-Boost shows the highest accurate results with an AUC value of 0.910 and RF with 0.906, and FR-EBF with 0.836 (refer to Table 3). These results are quite good as it is closer to unity or one. The ensemble of FR-EBF shows lower AUC values than the machine learning-based XG-Boost and Random Forest. Machine learning results may differ because the models used landslide and non-landslide features as training data, whereas FR-EBF results are derived solely from landslide data. The results may differ depending on the geographical location and the selection of landslide conditioning factors.

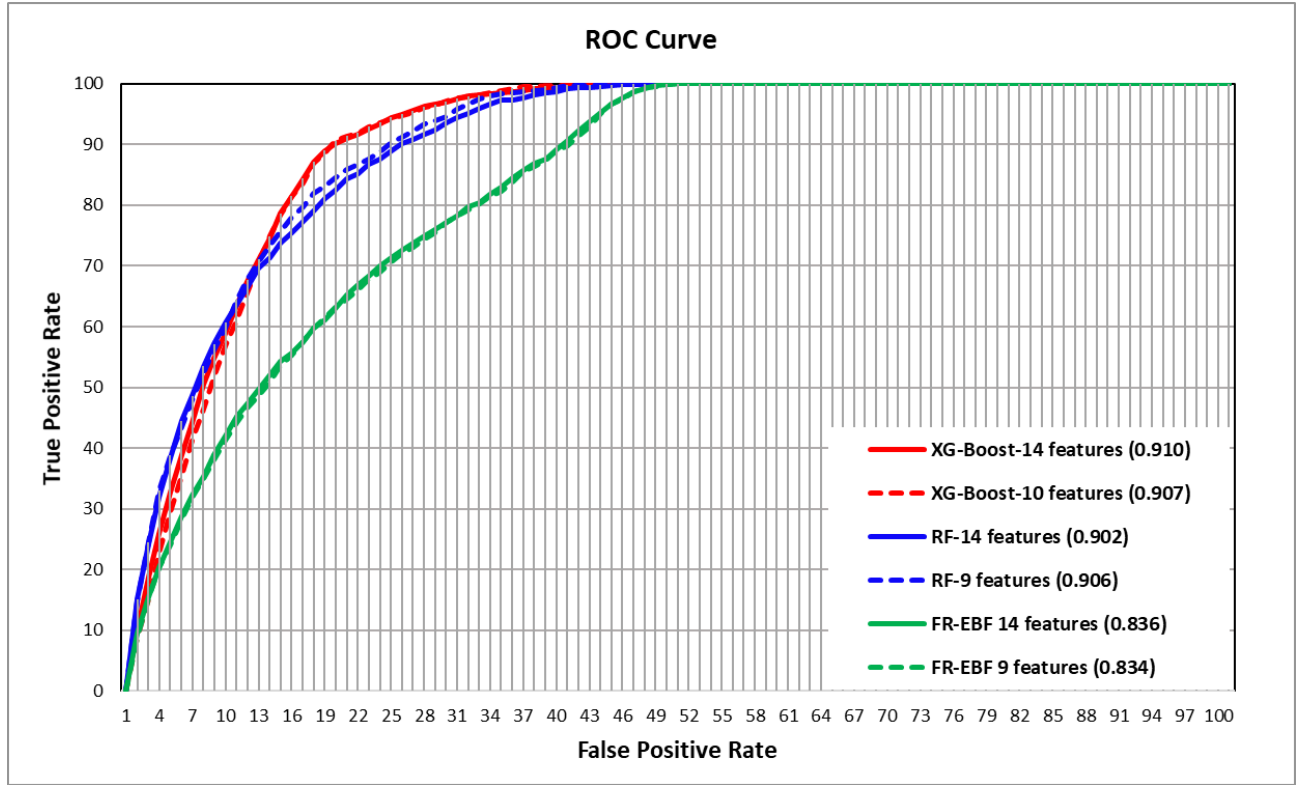


Figure 11. Testing for the performance of the statistical and machine learning models for LSM in Belluno province, Italy.

## 5.2 Relative Landslide Density (R-Index)

The relative landslide density index was also used to assess the accuracy of the LSMs (R-index). Equation (4) is used to get the R-index:

$$R = (n_i/N_i)/\Sigma(n_i/N_i) \times 100 \text{ (Eq.4)}$$

where  $N_i$  is the percentage of landslides in each susceptibility class and  $n_i$  is the percentage of area susceptible to landslides in each susceptibility class. Table 4 shows the quantile classification approach to classify the six landslide susceptibility maps into five susceptible classes. In comparison to the RF and FR-EBF models, the XG-Boost model with 14 and 10 features has a higher R-index for very high susceptibility classes. The R-index findings show

that FR EBF has a better R-index value for high susceptibility class than XG-Boost, which has the lowest R-index for high susceptibility class. FR-EBF has a higher r-index value for the high susceptibility class than the other three approaches. In addition, the R-index of FR-EBF is higher for the very low susceptible class. Table 4 shows the R-index values for susceptibility class in FR-EBF, RF, and XG-Boost, as well as plots of the same in figure 12.

Table 4: R-indices for the FR-EBF, RF, and XG-Boost models' landslide susceptibility mappings (LSMs).

Validation methods	Susceptibility class	Number of pixels	Area (m <sup>2</sup> )	Area (%) (ni)	Number of landslides	Landslide (%) (Ni)	R- index
FR-EBF-14							
Features	Very Low	21875	334248750	9.28	48	2.71	6
	Low	90000	570760000	15.85	171	9.66	13
	Moderate	165000	896709375	24.90	308	17.40	15
	High	263750	1026578125	28.50	460	25.99	20
	Very High	444375	773585000	21.48	783	44.24	45
FR-EBF-9							
Features	Very Low	19375	323332500	8.98	38	2.15	5
	Low	91875	541371875	15.03	179	10.11	15
	Moderate	153125	894758125	24.84	289	16.33	15
	High	276875	1041846875	28.93	480	27.12	21
	Very High	443750	800571875	22.23	784	44.29	44
RF-14							
Features	Very Low	6875	682346250	18.94	11	0.62	1
	Low	34375	658375000	18.28	55	3.11	4
	Moderate	75625	619031875	17.19	122	6.89	9

RF-9 Features	High	159375	749470625	20.81	264	14.92	17
	Very high	712500	892657500	24.78	1318	74.46	69
	Very Low	7500	735246875	20.41	12	0.68	1
	Low	30000	632679375	17.57	48	2.71	4
	Moderate	75000	581844375	16.15	120	6.78	10
	High	147500	692276250	19.22	245	13.84	17
	Very High	729375	959834375	26.65	1345	75.99	68
XG-Boost- 14 Features	Very Low	11250	1076978750	29.90	18	1.02	1
	Low	6875	330045625	9.16	11	0.62	3
	Moderate	11875	278243750	7.72	19	1.07	5
	High	11250	352568125	9.79	18	1.02	4
	Very High	947500	1564045000	43.42	1704	96.27	87
XG-Boost- 10 Features	Very Low	12500	1094226250	30.38	20	1.13	1
	Low	7500	297782500	8.27	12	0.68	3
	Moderate	8125	242914375	6.74	13	0.73	4
	High	15625	314181875	8.72	25	1.41	7
	Very High	945000	1652776250	45.89	1700	96.05	84

## 6. Discussion

Landslides are very dynamic in nature, meaning that their behaviour, movement, and spatial distribution changes over space and time. Therefore, it is important to analyse the significance of the conditioning factors that lead to landslide occurrences. The relevance of the conditioning features for LSM is essential to realize which of the features had the biggest impact on the

prediction of landslide occurrences. As not all conditioning factor maps be available globally, or sometimes even locally, due to reasons such as non-compliance in sharing data, data unavailability, erroneous data structure, and others, it can be worthwhile to understand which of the available conditioning factors play an important role in LSM. For example, topographical features derived from digital elevation models such as Elevation, Slope, aspect, Plan curvature, Profile curvature, TWI, TPI, TRI are available almost globally because of missions such as the Shuttle Radar Topography Mission (SRTM). Other features, such as distance to roads and drainage networks, that might have direct or indirect influence on the occurrence of landslides, can also be easily accessed through numerous open-source platforms. However, conditioning factor maps of rainfall data derived from rain gauge stations are not easily accessible and available. In this study, we used fourteen features for landslide susceptibility assessment and carried out the feature importance of the conditioning factors for traditional statistical ensemble model of FR-EBF and machine learning models of RF and XG-Boost. The feature selection approach from statistical model is dependent upon the landslide data and its relation to each feature and their classes. On the other hand, feature selection for machine learning models depends upon the landslide and non-landslide samples that are used to train the models. We used the in-built impurity feature importance algorithm to assess the importance of the features during the model training phases. Based on literature review for this sort of study, there is no standard threshold values available for discarding or selection of features for LSM. In this study, we used a trial-and-error approach to determine a threshold of 0.30 for the selection of conditioning factors used for landslide susceptibility for all the three models.

Feature importance algorithms used in this study are different, however there is similarity in the importance of the features in both statistical and machine learning algorithms (See [Figure 13](#)).

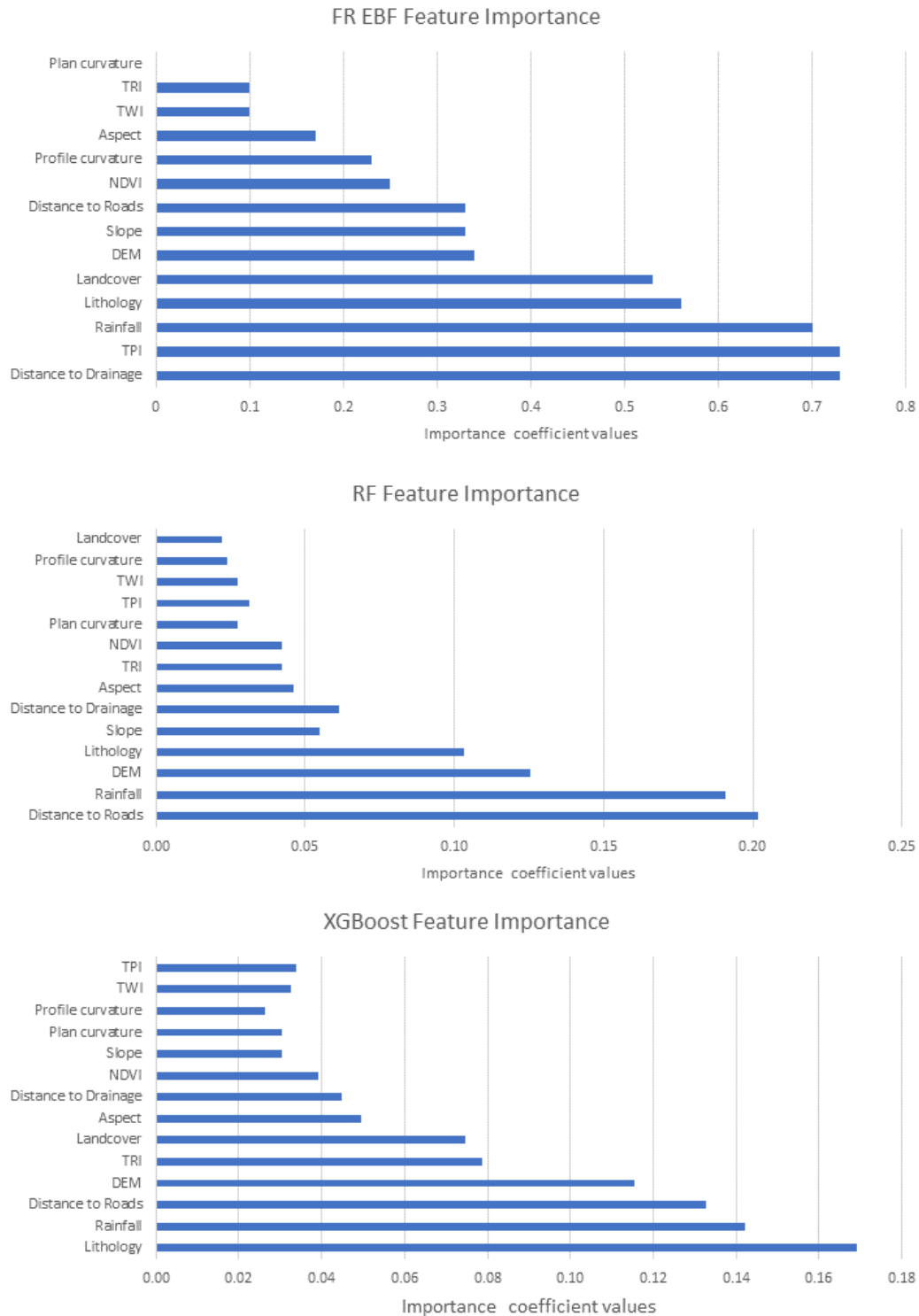


Figure 13: Importance of the features in both statistical and machine learning algorithms.

As we look at the figures 7, 8, and 9 in the enlarged region, we observe that there are not many differences despite removing the least important features. The reason for such observation can be linked to the lower impact of least important factors on overall LSM results.

Furthermore, there are several factors that determine the importance of features for carrying out LSM such as (1) completeness and quality of the landslide inventory dataset used for analysis, (2) mapping scale of the features maps like landcover, lithology, or other geological features. If the spatial locations of landslides in an inventory does not represent the ground truth phenomenon, then there can be negative impact of landslide input data for feature selection. Sampling methodology of landslide selection is important, there are various ways to use landslides in carrying out susceptibility assessment, many studies have used 70-30 ratio and others have used random sampling or K-fold sampling methods (Merghadi et al., 2018;Chen et al., 2018). One of the most important observations from this study was the exclusion of the "least important factors" in the context of LSM. The fact that despite removal of certain conditioning factors, we still get very good results or comparable results after removing them, this observation explains employing the important conditioning factors are enough for LSM.

The use of landslide samples along with non-landslide samples can affect the landslide feature importance as can be seen in results in this study. In the case of the statistical model, one of the reasons for the lower AUC performance can be accredited to the absence of the non-landslide samples. As the model was trained without non-landslide samples and simply trained with only landslide samples, the model's ability to discriminate between the non-landslide and landslide pixels is affected therefore, predicting landslide occurrences over non-landslide locations. Because of this reason, the statistical model exhibited homogeneous distribution of predicted landslide pixels (see figure 7). We used landslides and non-landslide samples for training the ML models which shows varying results from that of the statistical ensemble model (See figure 8 and 9). There is more homogeneous distribution of landslide susceptibility classes in statistical model results, but it is evident from the machine learning results that the non-landslide samples have a greater impact on final landslide susceptibility results.



We also attempted to investigate the relative changes in the susceptibility after removing the “least important” factors based on the study from Xiao et al. 2020. We made difference maps by subtracting the susceptibility maps modelled with 14 conditioning factors with susceptibility maps after removal of the c conditioning factors. The differences are calculated as: “FR-EBF 14-9”, “RF 14-9”, and “XG 14-10”. We wanted to assess if the obtained differences are random or follows a systematic pattern after removal of the factor maps. Because every susceptibility map's raster value is between 0 and 1, the comparison maps' values potentially vary from  $-1 \sim 1$ . The results of the differencing can be seen in Figure 12, and it is very clear from difference maps for all the three models that there is a random pattern after removal of least important conditioning factors. The removed conditioning factors for each of the models are:

1. Frequency Ratio Evidence Belief Function: Plan curvature, TRI, TWI, Aspect, Profile curvature.
2. Random Forest: Landcover, Profile curvature, TWI, TPI, Plan curvature
3. XG-Boost: Profile curvature, TWI, TPI, Plan curvature

Conditioning factor importance for all the models were similar such as Profile curvature, TWI, TPI, and Plan curvature, which were among the least important factors for landslide susceptibility analysis in our study. The impact of these four factors on landslide susceptibility results were not much as the ROC values and R-index values were not changed to a great extent. Also, the impact of removal of these factors is very evident from the differencing maps shown in Figure 12.

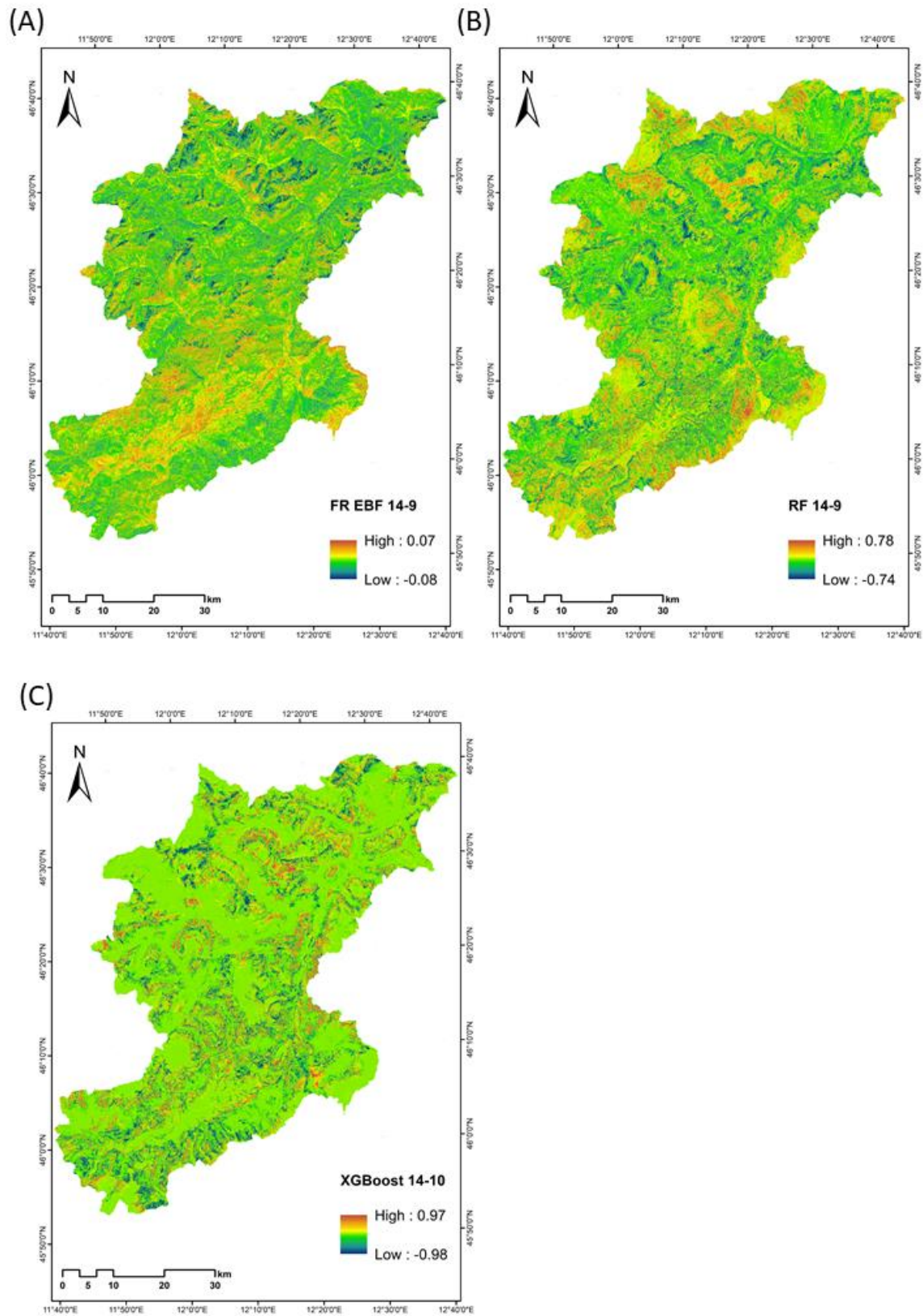


Figure 12. Three comparison maps (uniform legend: red–blue band from  $-1 \sim 1$ ).

## 7. Conclusions

In the current state-of-the-art approaches for LSM, the contemporary literature lays emphasis on different models for improving accuracy of landslide susceptibility against the test data. However, this study investigated how the conditioning factors affect the overall prediction of landslides in the context of northeast Italy, Belluno province. An important aspect of this study was to identify if at all, removing the “least important” conditioning factors in the modelling process affects the performance in predicting new unknown landslides.

As understood, ML models require conditioning factors as input for LSM, however, investing on the importance of the features (conditioning factors) could possibly provide a better understanding of landslide occurrences with respect to the available conditioning factor maps for LSM. This study indicates that various models behave differently with different features, whereby the same features that are important in one instance of a particular model, can be the least important in other models. Therefore, this study gives new insights towards the use of already available conditioning factor maps, without exhausting resources for generating other conditioning factor maps that might not be available.

In this study we also concluded that the landslides and non-landslides samples impacts the feature importance, especially in the ML models, and in contrast, the statistical model used only landslide samples. Therefore, it was found to be crucial in asserting a balance between the two data samples to avoid overfitting or underfitting. This study illustrates that feature selection is very important step of carrying out LSMs. We found that there are differences in the final LSMs derived from the statistical and ML models, which are attributed to the above-mentioned sample selection techniques.

This research introduces the importance of post-training feature importance algorithms for LSM. This approach can also be used to assess the susceptibility of other natural disasters. The results can eventually comment whether certain conditioning factors can be discarded while

modelling landslide occurrences. In many parts of the globe, the availability of data is scarce and therefore, with the ability to model landslides without relying on the conventional factors, we can still predict landslides spatially over a given region. Although there are certain drawbacks like (1) the same factor maps will not be available everywhere, (2) factors that are least important in one region might not repeat the same behaviour in other regions of the world, and (3) model capability changes with respect to different regions, the resulting susceptibility maps can still give quality information for local emergency relief measures, planning of disaster risk reduction, mitigation, and to evaluate potentially affected areas.

Funding: This research was funded by the Veneto Region, VAIA-LAND project, Research Unit UNIPD-GEO, Principal Investigator Mario Floris.

## References:

- Baglioni, A., Tosoni, D., De Marco, P., and Arziliro, L.: Analisi del dissesto da frana in Veneto, 2006.
- Baird, C.: Comparison of Risk Assessment Instruments in Juvenile Justice, 2013.
- Boretto, G., Crema, S., Marchi, L., Monegato, G., Arziliro, L., and Cavalli, M.: Assessing the effect of the Vaia storm on sediment source areas and connectivity storm in the Liera catchment (Dolomites), Copernicus Meetings, 2021.
- Brabb, E. E., Pampeyan, E. H., and Bonilla, M. G.: Landslide susceptibility in San Mateo County, California, Reston, VA, Report 360, 1972.
- Breiman, L.: Random Forests, Machine Learning, 45, 5-32, 10.1023/A:1010933404324, 2001.
- Can, R., Kocaman, S., and Gokceoglu, C.: A Comprehensive Assessment of XGBoost Algorithm for Landslide Susceptibility Mapping in the Upper Basin of Ataturk Dam, Turkey, Applied Sciences, 11, 4993, 2021.
- Castellanos Abella, E. A., and Van Westen, C. J.: Qualitative landslide susceptibility assessment by multicriteria analysis: A case study from San Antonio del Sur, Guantánamo, Cuba, Geomorphology, 94, 453-466, 10.1016/j.geomorph.2006.10.038, 2008.
- Catani, F., Lagomarsino, D., Segoni, S., and Tofani, V.: Landslide susceptibility estimation by random forests technique: sensitivity and scaling issues, Natural Hazards and Earth System Sciences, 13, 2815-2831, 10.5194/nhess-13-2815-2013, 2013.
- Chacón, J., Irigaray, C., Fernández, T., and El Hamdouni, R.: Engineering geology maps: landslides and geographical information systems, Bulletin of Engineering Geology and the Environment, 65, 341-411, 10.1007/s10064-006-0064-z, 2006.
- Chen, T., Trinder, J. C., and Niu, R.: Object-oriented landslide mapping using ZY-3 satellite imagery, random forest and mathematical morphology, for the Three-Gorges Reservoir, China, Remote sensing, 9, 333, 2017.

575 Chen, W., Peng, J. B., Hong, H. Y., Shahabi, H., Pradhan, B., Liu, J. Z., Zhu, A. X., Pei, X. J.,  
 576 and Duan, Z.: Landslide susceptibility modelling using GIS-based machine learning techniques  
 577 for Chongren County, Jiangxi Province, China, *Science of the Total Environment*, 626, 1121-  
 578 1135, 10.1016/j.scitotenv.2018.01.124, 2018.  
 579 Chung, C.-J. F., and Fabbri, A. G.: Validation of Spatial Prediction Models for Landslide  
 580 Hazard Mapping, *Natural Hazards*, 30, 451-472, 10.1023/B:NHAZ.00000007172.62651.2b,  
 581 2003.  
 582 Compagnoni, B., Galluzzo, F., Bonomo, R., and Tacchia, D.: Carta geologica d'Italia,  
 583 Dipartimento difesa del suolo, 2005.  
 584 Corò, D., Galgaro, A., Fontana, A., and Carton, A.: A regional rockfall database: the Eastern  
 585 Alps test site, *Environmental Earth Sciences*, 74, 1731-1742, 10.1007/s12665-015-4181-5,  
 586 2015.  
 587 Dahal, R. K., Hasegawa, S., Nonomura, A., Yamanaka, M., Masuda, T., and Nishino, K.: GIS-  
 588 based weights-of-evidence modelling of rainfall-induced landslides in small catchments for  
 589 landslide susceptibility mapping, *Environmental Geology*, 54, 311-324, 10.1007/s00254-007-  
 590 0818-3, 2008.  
 591 Dai, F. C., Lee, C. F., and Ngai, Y. Y.: Landslide risk assessment and management: an  
 592 overview, *Engineering Geology*, 64, 65-87, [https://doi.org/10.1016/S0013-7952\(01\)00093-X](https://doi.org/10.1016/S0013-7952(01)00093-X),  
 593 2002.  
 594 Desiato, F., Lena, F., Baffo, F., Suatoni, B., Toreti, A., di Ecologia Agraria, U. C., and  
 595 Romagna, A. E.: Indicatori del clima in Italia, APAT, Roma, 2005.  
 596 Doglioni, C.: Thrust tectonics examples from the Venetian Alps, 1990.  
 597 Dunning, S., Massey, C., and Rosser, N.: Structural and geomorphological features of  
 598 landslides in the Bhutan Himalaya derived from terrestrial laser scanning, *Geomorphology*,  
 599 103, 17-29, 2009.  
 600 Dury, G.: Hillslope form and Process. M.A. Carson and M.J. Kirkby, 1972. Cambridge  
 601 University Press, London, vii + 475 pp., £ 6.60, 1972,  
 602 Ercanoglu, M., and Gokceoglu, C.: Assessment of landslide susceptibility for a landslide-prone  
 603 area (north of Yenice, NW Turkey) by fuzzy approach, *Environmental Geology*, 41, 720-730,  
 604 10.1007/s00254-001-0454-2, 2002.  
 605 Floris, M., Iafelice, M., Squarzoni, C., Zorzi, L., De Agostini, A., and Genevois, R.: Using  
 606 online databases for landslide susceptibility assessment: an example from the Veneto Region  
 607 (northeastern Italy), *Nat. Hazards Earth Syst. Sci.*, 11, 1915-1925, 10.5194/nhess-11-1915-  
 608 2011, 2011.  
 609 Forzieri, G., Pecchi, M., Girardello, M., Mauri, A., Klaus, M., Nikolov, C., Rüetschi, M.,  
 610 Gardiner, B., Tomaščík, J., Small, D., Nistor, C., Jonikavicius, D., Spinoni, J., Feyen, L.,  
 611 Giannetti, F., Comino, R., Wolynski, A., Pirotti, F., Maistrelli, F., Savulescu, I., Wurrpillot-  
 612 Lucas, S., Karlsson, S., Zieba-Kulawik, K., Strejczek-Jazwinska, P., Mokroš, M., Franz, S.,  
 613 Krejci, L., Haidu, I., Nilsson, M., Wezyk, P., Catani, F., Chen, Y. Y., Luyssaert, S., Chirici,  
 614 G., Cescatti, A., and Beck, P. S. A.: A spatially explicit database of wind disturbances in  
 615 European forests over the period 2000–2018, *Earth Syst. Sci. Data*, 12, 257-276, 10.5194/essd-  
 616 12-257-2020, 2020.  
 617 Froude, Melanie J., and David N. Petley. 2018. 'Global fatal landslide occurrence from 2004  
 618 to 2016', *Natural Hazards and Earth System Sciences*, 18: 2161-81.  
 619 Gariano, S. L., Verini Supplizi, G., Ardizzone, F., Salvati, P., Bianchi, C., Morbidelli, R., and  
 620 Saltalippi, C.: Long-term analysis of rainfall-induced landslides in Umbria, central Italy,  
 621 *Natural Hazards*, 106, 2207-2225, 10.1007/s11069-021-04539-6, 2021.  
 622 Ghorbanzadeh, O., Rostamzadeh, H., Blaschke, T., Gholaminia, K., and Aryal, J.: A new GIS-  
 623 based data mining technique using an adaptive neuro-fuzzy inference system (ANFIS) and k-

fold cross-validation approach for land subsidence susceptibility mapping, *Natural Hazards*, 94, 497-517, 10.1007/s11069-018-3449-y, 2018.

Glade, T., Anderson, M. G., and Crozier, M. J.: *Landslide hazard and risk*, John Wiley & Sons, 2006.

Goetz, J. N., Brenning, A., Petschko, H., and Leopold, P.: Evaluating machine learning and statistical prediction techniques for landslide susceptibility modeling, *Computers & Geosciences*, 81, 1-11, 10.1016/j.cageo.2015.04.007, 2015.

Guzzetti, F., Reichenbach, P., Ardizzone, F., Cardinali, M., and Galli, M.: Estimating the quality of landslide susceptibility models, *Geomorphology*, 81, 166-184, 10.1016/j.geomorph.2006.04.007, 2006.

Huang, F., Chen, J., Du, Z., Yao, C., Huang, J., Jiang, Q., Chang, Z., and Li, S.: Landslide Susceptibility Prediction Considering Regional Soil Erosion Based on Machine-Learning Models, *ISPRS International Journal of Geo-Information*, 9, 377, 2020.

Iadanza, C., Trigila, A., Starace, P., Dragoni, A., Biondo, T., and Roccisano, M.: IdroGEO: A Collaborative Web Mapping Application Based on REST API Services and Open Data on Landslides and Floods in Italy, *ISPRS International Journal of Geo-Information*, 10, 89, 2021.

Komac, M.: A landslide susceptibility model using the Analytical Hierarchy Process method and multivariate statistics in perialpine Slovenia, *Geomorphology*, 74, 17-28, 10.1016/j.geomorph.2005.07.005, 2006.

Lee, S.: Landslide detection and susceptibility mapping in the Sagimakri area, Korea using KOMPSAT-1 and weight of evidence technique, *Environmental Earth Sciences*, 70, 3197-3215, 10.1007/s12665-013-2385-0, 2013.

Linden, A.: Measuring diagnostic and predictive accuracy in disease management: an introduction to receiver operating characteristic (ROC) analysis, *Journal of evaluation in clinical practice*, 12, 132-139, 2006.

Liu, L.-L., Yang, C., and Wang, X.-M.: Landslide susceptibility assessment using feature selection-based machine learning models, *Geomechanics and Engineering*, 25, 1-16, 2021.

Melville, B., Lucieer, A., and Aryal, J.: Object-based random forest classification of Landsat ETM+ and WorldView-2 satellite imagery for mapping lowland native grassland communities in Tasmania, Australia, *International journal of applied earth observation and geoinformation*, 66, 46-55, 2018.

Merghadi, A., Abderrahmane, B., and Tien Bui, D.: Landslide Susceptibility Assessment at Mila Basin (Algeria): A Comparative Assessment of Prediction Capability of Advanced Machine Learning Methods, *ISPRS International Journal of Geo-Information*, 7, 10.3390/ijgi7070268, 2018.

Meten, M., PrakashBhandary, N., and Yatabe, R.: Effect of Landslide Factor Combinations on the Prediction Accuracy of Landslide Susceptibility Maps in the Blue Nile Gorge of Central Ethiopia, *Geoenvironmental Disasters*, 2, 9, 10.1186/s40677-015-0016-7, 2015.

Micheletti, N., Foresti, L., Robert, S., Leuenberger, M., Pedrazzini, A., Jaboyedoff, M., and Kanevski, M.: Machine Learning Feature Selection Methods for Landslide Susceptibility Mapping, *Mathematical Geosciences*, 46, 33-57, 10.1007/s11004-013-9511-0, 2014.

Mondal, S., and Maiti, R.: Integrating the analytical hierarchy process (AHP) and the frequency ratio (FR) model in landslide susceptibility mapping of Shiv-khola watershed, Darjeeling Himalaya, *International Journal of Disaster Risk Science*, 4, 200-212, 2013.

Pham, B. T., Tien Bui, D., Pourghasemi, H. R., Indra, P., and Dholakia, M. B.: Landslide susceptibility assessment in the Uttarakhand area (India) using GIS: a comparison study of prediction capability of naïve bayes, multilayer perceptron neural networks, and functional trees methods, *Theoretical and Applied Climatology*, 128, 255-273, 10.1007/s00704-015-1702-9, 2015.



Pham, B. T., Tien Bui, D., and Prakash, I.: Bagging based Support Vector Machines for spatial prediction of landslides, *Environmental Earth Sciences*, 77, 146, 10.1007/s12665-018-7268-y, 2018.

Pourghasemi, H. R., Pradhan, B., and Gokceoglu, C.: Application of fuzzy logic and analytical hierarchy process (AHP) to landslide susceptibility mapping at Haraz watershed, Iran, *Natural hazards*, 63, 965-996, 2012.

Pradhan, B.: Landslide susceptibility mapping of a catchment area using frequency ratio, fuzzy logic and multivariate logistic regression approaches, *Journal of the Indian Society of Remote Sensing*, 38, 301-320, 10.1007/s12524-010-0020-z, 2010.

Raja, N. B., Çiçek, I., Türkoğlu, N., Aydın, O., and Kawasaki, A.: Landslide susceptibility mapping of the Sera River Basin using logistic regression model, *Natural Hazards*, 85, 1323-1346, 10.1007/s11069-016-2591-7, 2017.

Reichenbach, P., Rossi, M., Malamud, B. D., Mihir, M., and Guzzetti, F.: A review of statistically-based landslide susceptibility models, *Earth-Science Reviews*, 180, 60-91, 10.1016/j.earscirev.2018.03.001, 2018.

Riley, S. J., DeGloria, S. D., and Elliot, R.: Index that quantifies topographic heterogeneity, *intermountain Journal of sciences*, 5, 23-27, 1999.

Rossi, M., Guzzetti, F., Salvati, P., Donnini, M., Napolitano, E., and Bianchi, C.: A predictive model of societal landslide risk in Italy, *Earth-Science Reviews*, 196, 102849, <https://doi.org/10.1016/j.earscirev.2019.04.021>, 2019.

Ruff, M. and K Czurda. 2008. 'Landslide susceptibility analysis with a heuristic approach in the Eastern Alps (Vorarlberg, Austria)', *Geomorphology*, 94: 314-24.

Sahin, E. K.: Assessing the predictive capability of ensemble tree methods for landslide susceptibility mapping using XGBoost, gradient boosting machine, and random forest, *SN Applied Sciences*, 2, 1308, 10.1007/s42452-020-3060-1, 2020.

Sauro, F., Zampieri, D., and Filipponi, M.: Development of a deep karst system within a transpressional structure of the Dolomites in north-east Italy, *Geomorphology*, 184, 51-63, <https://doi.org/10.1016/j.geomorph.2012.11.014>, 2013.

Schönborn, G.: Balancing cross sections with kinematic constraints: The Dolomites (northern Italy), *Tectonics*, 18, 527-545, 1999.

Segoni, S., Pappafico, G., Luti, T., & Catani, F. (2020). Landslide susceptibility assessment in complex geological settings: Sensitivity to geological information and insights on its parameterization. *Landslides*, 17(10), 2443-2453.

Senouci, R., Taibi, N.-E., Teodoro, A. C., Duarte, L., Mansour, H., and Yahia Meddah, R.: GIS-Based Expert Knowledge for Landslide Susceptibility Mapping (LSM): Case of Mostaganem Coast District, West of Algeria, *Sustainability*, 13, 630, 2021.

Shahabi, H., Khezri, S., Ahmad, B. B., and Hashim, M.: Landslide susceptibility mapping at central Zab basin, Iran: a comparison between analytical hierarchy process, frequency ratio and logistic regression models, *Catena*, 115, 55-70, 2014.

Shahabi, H., and Hashim, M.: Landslide susceptibility mapping using GIS-based statistical models and Remote sensing data in tropical environment, *Scientific reports*, 5, 9899, 2015.

Stanley, T. A., Kirschbaum, D. B., Benz, G., Emberson, R. A., Amatya, P. M., Medwedeff, W., and Clark, M. K.: Data-Driven Landslide Nowcasting at the Global Scale, *Frontiers in Earth Science*, 9, 10.3389/feart.2021.640043, 2021.

Trigila, A., Iadanza, C., and Spizzichino, D.: Quality assessment of the Italian Landslide Inventory using GIS processing, *Landslides*, 7, 455-470, 10.1007/s10346-010-0213-0, 2010.

Trigila, A., and Iadanza, C.: Landslides and floods in Italy: hazard and risk indicators - Summary Report 2018, 2018.

721 van Westen, C. J., Castellanos, E., and Kuriakose, S. L.: Spatial data for landslide  
722 susceptibility, hazard, and vulnerability assessment: An overview, *Engineering Geology*, 102,  
723 112-131, 10.1016/j.enggeo.2008.03.010, 2008.

724 Youssef, A. M., and Pourghasemi, H. R.: Landslide susceptibility mapping using machine  
725 learning algorithms and comparison of their performance at Abha Basin, Asir Region, Saudi  
726 Arabia, *Geoscience Frontiers*, 12, 639-655, 10.1016/j.gsf.2020.05.010, 2021.

727

728